



**KfK 4287
EUR 10537 e
August 1987**

Thermomechanical Analysis of Different First Wall Designs for the Helium Cooled Pebble Bed Canister Blanket for NET

**G. Sordon
Institut für Neutronenphysik und Reaktortechnik
Projekt Kernfusion**

Kernforschungszentrum Karlsruhe

KERNFORSCHUNGSZENTRUM KARLSRUHE
Institut für Neutronenphysik und Reaktortechnik
Projekt Kernfusion

KfK 4287

EUR 10537e

Thermomechanical analysis of different first wall designs
for the helium cooled pebble bed canister blanket for NET

Giancarlo Sordon

Kernforschungszentrum Karlsruhe GmbH, Karlsruhe

Als Manuskript vervielfältigt
Für diesen Bericht behalten wir uns alle Rechte vor

Kernforschungszentrum Karlsruhe GmbH
Postfach 3640, 7500 Karlsruhe 1

ISSN 0303-4003

ABSTRACT

A 2-D thermomechanical analysis of He-cooled first wall designs with radiatively cooled protection tiles was performed with the FE-code ABAQUS. These designs were suggested for the KfK-NET blanket concept with ceramic breeder material. The calculated temperature distributions for the tiles and for the underlying steel structure are reported. In addition the stress distributions for the steel structure are presented. All calculations were performed for steady state conditions. The results show that a helium cooled first wall for heat fluxes up to 40 W/cm^2 seems feasible.

Thermodynamische Analyse von verschiedenen Erste-Wand-Konzepten für das heliumgekühlte Kugelschüttung-Kanister-Blanket für NET

ZUSAMMENFASSUNG

Eine zweidimensionale thermomechanische Analyse für verschiedene Erste-Wand-Konzepte wurde mit dem Programm ABAQUS durchgeführt. Die für das keramische KfK-NET Blanket vorgeschlagenen Entwürfe bestehen aus heliumgekühlten Rohren mit aufgesteckten Graphitziegeln. Hier werden die im stationären Zustand berechneten Temperaturfelder für die Ziegel und Temperatur- und Spannungsfelder für die unterliegende Stahlstruktur gezeigt. Diese Rechnungen zeigen, daß eine thermische Wandbelastung von 40 W/cm^2 mit einer heliumgekühlten Ersten Wand beherrschbar ist.

TABLE OF CONTENTS

1. Introduction	1
2. Features of the designs	1
3. Calculation models, boundary conditions and material properties . .	2
4. Results	3
5. Conclusions	4
References	5

LIST OF ILLUSTRATIONS

Figure 1. Vertical cut through plasma chamber of NET-KfK design with ceramic breeder material	8
Figure 2. Heat transmission in tile-protected helium cooled first wall design	9
Figure 3. First wall designs with the tubes brazed inside the canisters	10
Figure 4. First wall designs with the tubes welded outside the canisters	11
Figure 5. Mesh schematization for the geometries 1, 2 and 3.	12
Figure 6. Mesh schematization for the geometries 4 and 5.	13
Figure 7. Boundary conditions for the calculation model 1	14
Figure 8. Boundary conditions for the calculation models 2.1 and 2.2	15
Figure 9. Boundary conditions for the calculation models 3.1 and 3.2	16
Figure 10. Boundary conditions for the calculation models 4. and 5.	17
Figure 11. Temperature contours in tile for the calculation 1.	18
Figure 12. Temperature contours in steel for the calculation 1.	19
Figure 13. Equivalent von Mises stress contours in steel for the calculation 1.	20
Figure 14. Temperature contours in tile for the calculation 2.1	21
Figure 15. Temperature contours in steel for the calculation 2.1	22
Figure 16. Equivalent von Mises stress contours in steel for the calculation 2.1	23
Figure 17. Temperature contours in tile for the calculation 2.2	24
Figure 18. Temperature contours in steel for the calculation 2.2	25
Figure 19. Equivalent von Mises stress contours in steel for the calculation 2.2	26
Figure 20. Temperature contours in tile for the calculation 3.1	27
Figure 21. Temperature contours in steel for the calculation 3.1	28
Figure 22. Equivalent von Mises stress contours in steel for the calculation 3.1	29
Figure 23. Temperature contours in tile for the calculation 3.2	30
Figure 24. Temperature contours in steel for the calculation 3.2	31
Figure 25. Equivalent von Mises stress contours in steel for the calculation 3.2	32
Figure 26. Temperature contours in tile for the calculation 4.	33
Figure 27. Temperature contours in steel for the calculation 4.	34
Figure 28. Equivalent von Mises stress contours in steel for the calculation 4.	35

Figure 29. Temperature contours in tile for the calculation 5. . . .	36
Figure 30. Temperature contours in steel for the calculation 5. . . .	37
Figure 31. Equivalent von Mises stress contours in steel for the calculation 5.	38

1. INTRODUCTION

For the KfK-NET blanket concept /1/, based on self-supporting pebble bed canisters surrounded by a separately cooled first wall vessel (Figure 1 on page 10), different He-cooled first wall designs were suggested /2/. These designs are characterized by graphite protection tiles fitted between cooling tubes. The heat flux from the plasma is transferred from the tiles to the cooling tubes by thermal radiation (Figure 2 on page 11). The finite element computer code ABAQUS /3/ was used to calculate temperature distributions in the graphite tiles.¹ It was also used to calculate temperature and thermal stress distributions in the underlying steel structure.

2. FEATURES OF THE DESIGNS

Five different designs were considered :

- Three configurations with the tubes inside the canisters were proposed. These configurations maintain the principle of double containment of the helium coolant (Figure 3 on page 12). In the reference design the plasma-facing side of the first wall is corrugated to form rails between which the graphite tiles are fitted (Figure 3.a) The cooling tubes are brazed to the inside of the canisters on this corrugated sheet. The thermal analysis (see section 4.Results) shows that in this reference design the heat flux from plasma cannot be over 10 W/cm^2 without exceeding the maximum allowable stress in the steel. This model can be improved by brazing a piece of steel on the tube inside the canisters

¹ The programmes FEMGEN /4/and FEMVIEW/5/ were also used : the former to prepare the inputs for ABAQUS, the latter to plot the results

(Figure 3.b) or by closing completely the cooling tubes between the corrugate sheet and an underlying plate brazed to them (Figure 3.c).

- Two other configurations with the tubes welded to the outside of the canisters were also proposed (Figure 4 on page 13). These proposals do not allow double containment of the pressurized helium coolant. The two configurations differ from one another in diameter and thickness of the cooling tubes ($d=22$ mm, $s=2$ mm in the geometry 4, $d=15$ mm, $s=1.5$ mm in the geometry 5), distance between the tubes (30 mm or 23 mm respectively) and total height (45 mm or 37 mm).

In all these design proposals helium at 6 MPa is used as coolant, and there is a 15 mm thick graphite erosion layer.

3. CALCULATION MODELS, BOUNDARY CONDITIONS AND MATERIAL PROPERTIES

The adopted finite element meshes for the five different geometries are shown in Figure 5 on page 14 and Figure 6 on page 15. Meshes (not shown in these figures) for the radiative heat transfer calculation are also assumed along the gap between the graphite tile and the steel structure. The emissivities governing this heat transfer are taken constant along the graphite surface ($\epsilon_G = 0.9$) but they are varied along the stainless steel surface.

As indicated in Figure 2 on page 11 the heat input comes from a surface heat flux \dot{q}'' and from the volumetric heat source \dot{q}_S''' in steel and \dot{q}_G''' in graphite. The convective heat transfer boundary condition is characterized by a coolant temperature T_{He} and by a heat transfer coefficient h between tube wall and coolant helium. The boundary conditions for the different calculations, taken from reference /2/, are related to the outboard blanket and they are shown in Figure 7 to Figure 10.

To calculate thermal stresses within the steel cross-section the generalized plane strain theory was used. This theory assumes that the model lies between two planes (normal to the axis of the tubes in this case) which may

move as rigid bodies relative to each other. No plastic deformation was considered, the primary stresses due to the coolant pressure in tubes were included in the calculation. The assumed mechanical constraints are :

- suppressed bending in the direction of the tubes,
- no rotation of the middle plane between two tubes,
- the plane through the axis of a tube and normal to the plasma facing side of the graphite tiles is a plane of symmetry.

The thermomechanical properties of the materials are specified in table I.

4. RESULTS

Temperature and von Mises equivalent stress contours for the different calculations are shown in Figure 41 to Figure 31. The resulting maximum temperatures and stresses are shown in table II together with the assumed boundary conditions. To evaluate the results we have considered, as a rough orientation, the following limiting values :

- a maximum allowable graphite temperature of 1800°C,
- a maximum allowable von Mises equivalent stress in the steel of 300 MPa.

In geometry 1 (calculation 1., Figure 12) there is a 160°C steady state temperature difference in the steel structure between the hottest point at the symmetry line away from the tube and the coldest point at the inside of the tube. In this latter point the stress reaches the limiting value at a heat flux from the plasma of only 10 W/cm². Adding a piece of steel to the tubes inside the canisters as proposed in geometries 2 and 3 remarkably reduces the maximum equivalent stresses. The maximum values for the equivalent stresses in geometries 2 and 3 are about 300 MPa. Geometry 3 has slightly lower stresses than geometry 2. Parametrically reducing the thermal emis-

sivity along the tube wall (calculation 2.2) reduces the maximum stresses, but on the other hand it increases the maximum graphite temperature. Also increasing the volumetric heat source in graphite, naturally, increases the value of the maximum stresses (see case 3.2).

For the geometry 4, which has the cooling tubes outside the canisters, the maximum stress (Figure 28) exceeds far the limiting value at a heat flux from the plasma of 20 W/cm^2 . Reducing the diameter, the distance between tubes and the steel emissivity on the supporting plate as proposed in the geometry 5, one reaches the limiting requirements with a surface heat flux at the graphite tiles of 40 W/cm^2 (Figures 29, 30 and 31).

5. CONCLUSIONS

From the performed thermomechanical analysis we can conclude that a helium cooled first wall design with radiatively cooled protection graphite tiles for heat fluxes up to 40 W/cm^2 seems feasible. In the design with closed cooling tubes, inside the canisters, (geometry 2 and 3, Figure 3) the maximum graphite temperature and steel equivalent stresses are a little over the limiting values for a heat flux from the plasma of 40 W/cm^2 . The reference design (geometry 1, Figure 3), in which the cooling tubes are only brazed to the inside of the canisters, will not work for such a heat flux.

The proposals with the tubes welded to the outside of the first wall vessel, suffer from the lack of double containment but have more flexibility. For this configurations a proper choice of the design parameters (geometry 5, Figure 4) allows a maximum heat flux from the plasma of 40 W/cm^2 .

Acknowledgement

The author thanks Mr. E. Diegele and Miss G. Schweinfurther for helping him during his early attempts to use the code ABAQUS.

REFERENCES

- /1/ M.Dalle Donne, U.Fischer, G.Sordon, E.Bojarsky, H.Reiser, P.Norajita, E.Bogusch: 'Pebble Bed Canister : A Ceramic Breeder Blanket with Helium Cooling for NET' 14th SOFT, Avignon, 8-12th September 1986.
- /2/ M.Dalle Donne: 'Private communication' Januar 1987.
- /3/ 'ABAQUS - A General Purpose Linear and non Linear Finite Element Code, Update to Version 4.5' Hibbit Karlsson and Sorensen, Inc.
- /4/ 'FEMGEN - A General Finite Element Code Mesh Generator, Update to Version 8.5' IKO-Software Service Gmbh, Albstadtweg 10, 7000 Stuttgart 80
- /5/ 'FEMVIEW - A General Finite Element Analysis Post-processor, Update to Version 3.5' IKO-Software Service Gmbh, Albstadtweg 10, 7000 Stuttgart 80

Table I : Material properties

member	Temperature (°C)	Thermal conductivity (W/m°C)	Thermal expansion coefficient (10 ⁻⁶ /K)	Young's modulus (10 ⁵ MPa)	Poisson's ratio
Steel	100.	15.6	0.166	1.86	0.3
	200.	17.0	0.171	1.78	
	300.	18.4	0.175	1.70	
	400.	19.7	0.178	1.61	
	500.	21.1	0.181	1.53	
Graphite	500.	64.6			
	600.	56.4			
	700.	51.7			
	800.	47.0			
	900.	43.5			
	1000.	41.1			
	1200.	36.4			
	1500.	31.7			
2000.	25.8				

Table II : Boundary conditions and maximum temperatures and stresses for the different calculations

models	1.	2.1	2.2	3.1	3.2	4.	5.
geometry	1	2	2	3	3	4	5
\dot{q}'' (W/cm ²)	10.	40.	40.	40.	40.	20.	40.
\dot{q}'''_G (W/cm ³)	6.3	6.3	6.3	6.3	9.4	9.4	8.96
\dot{q}'''_S (W/cm ³)	11.2	11.2	11.2	11.2	11.2	11.2	11.73
ϵ_G	0.9	0.9	0.9	0.9	0.9	0.9	0.9
ϵ_S	0.9/0.3*	0.9	0.6/0.9*	0.6/0.9*	0.6/0.9*	0.9	0.9/0.25*
T _{He} (°C)	264.	264.	264.	264.	264.	264.	251.
h (W/cm ² °C)	0.234	0.234	0.234	0.234	0.234	0.234	0.381
T _G ^{max} (°C)	1150.	1660.	1790.	1790.	1880.	1350.	1640.
T _S ^{min} (°C)	273.	333.	338.	342.	348.	359.	339.
T _S ^{max} (°C)	432.	538.	522.	520.	555.	623.	502.
$\sigma_{\text{von MISES},S}^{\text{max}}$ (MPa)	297.	325.	278.	266.	307.	398.	280.

* There are two different values of the emissivity along the steel surface (see Fig. 8, 9 and 10).

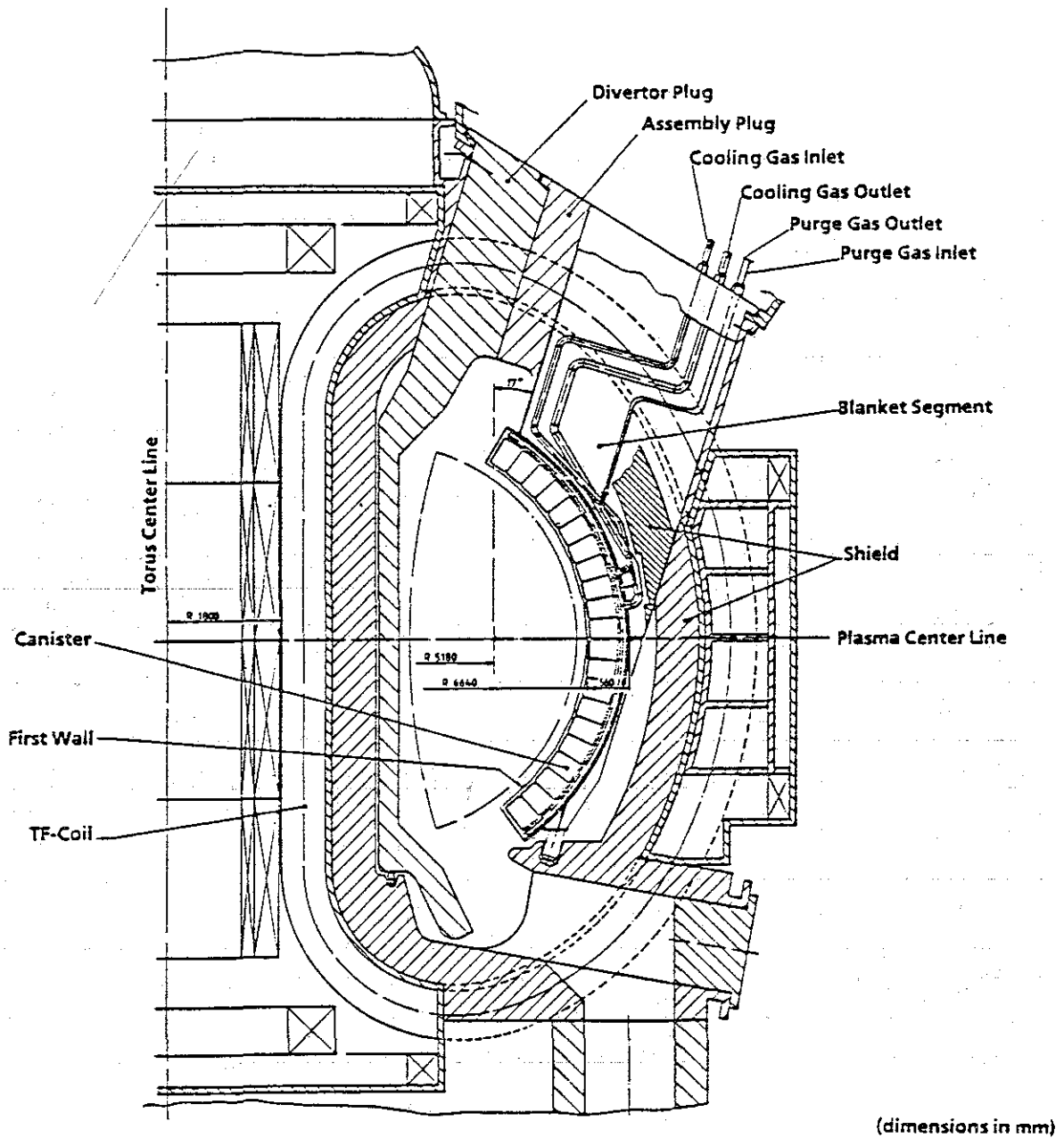


Figure 1. Vertical cut through plasma chamber of NET-KfK design with ceramic breeder material

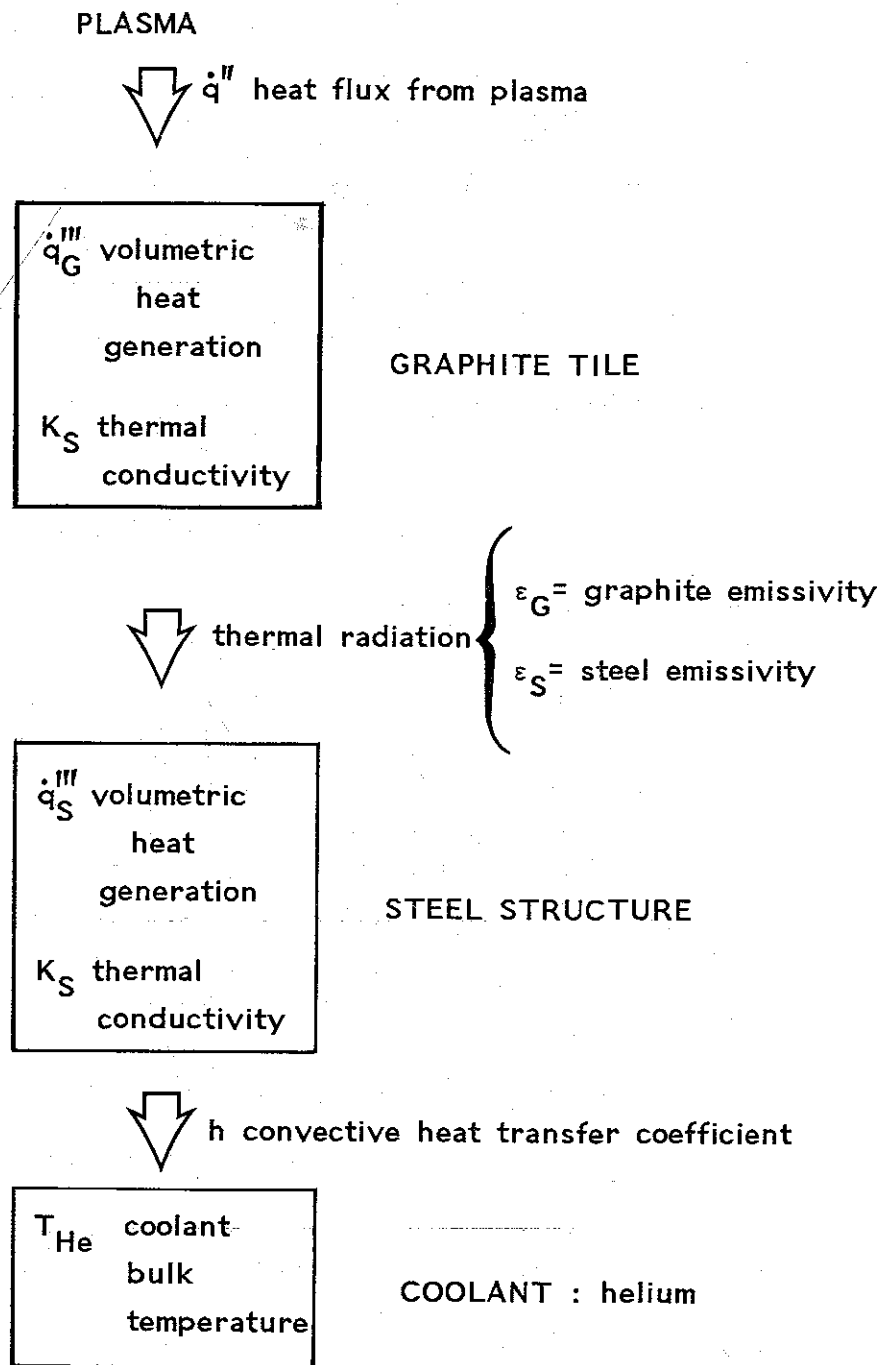


Figure 2. Heat transmission in tile-protected helium cooled first wall design

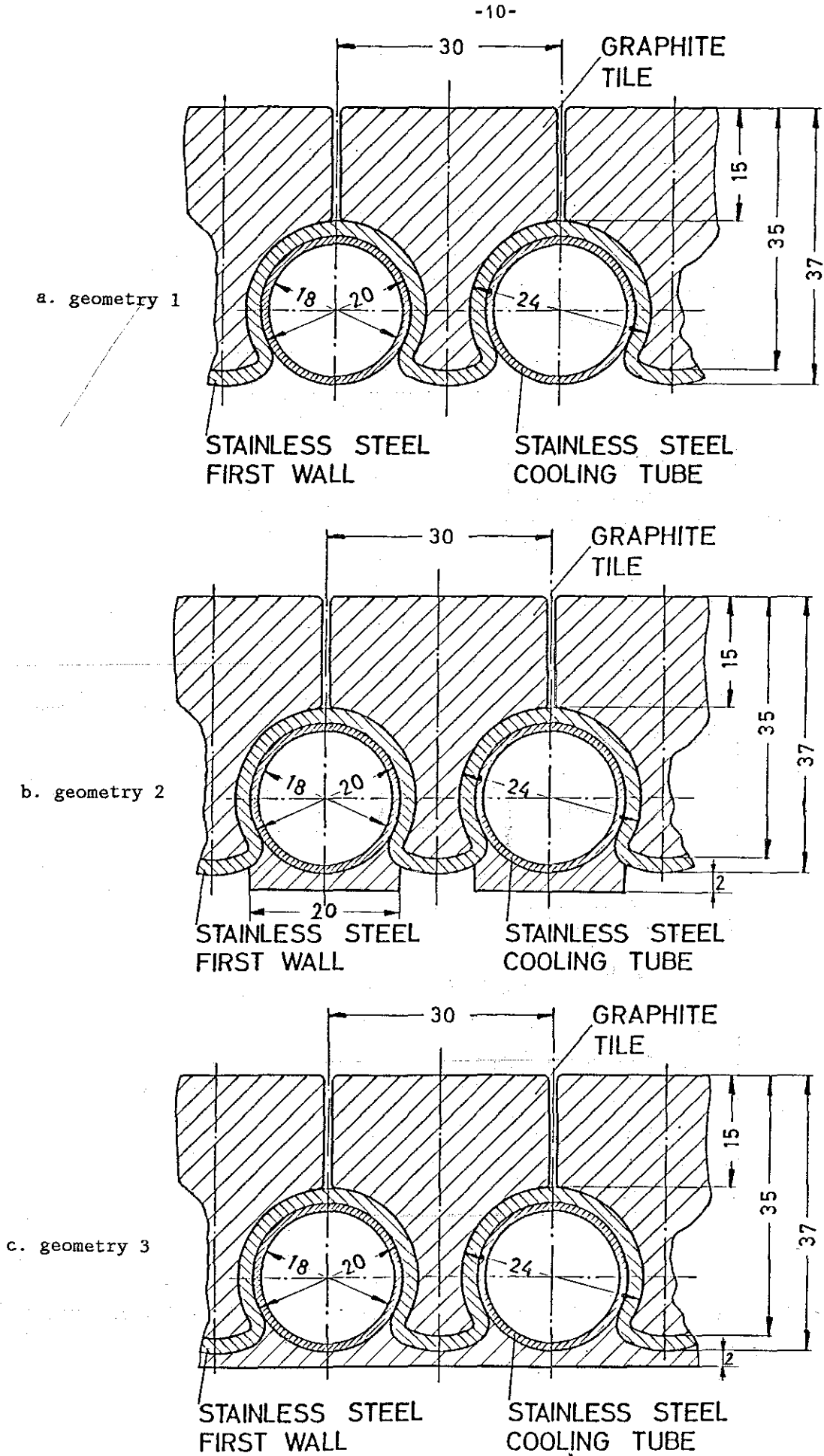


Figure 3. First wall designs with the tubes brazed inside the canisters (dimensions in millimeters).

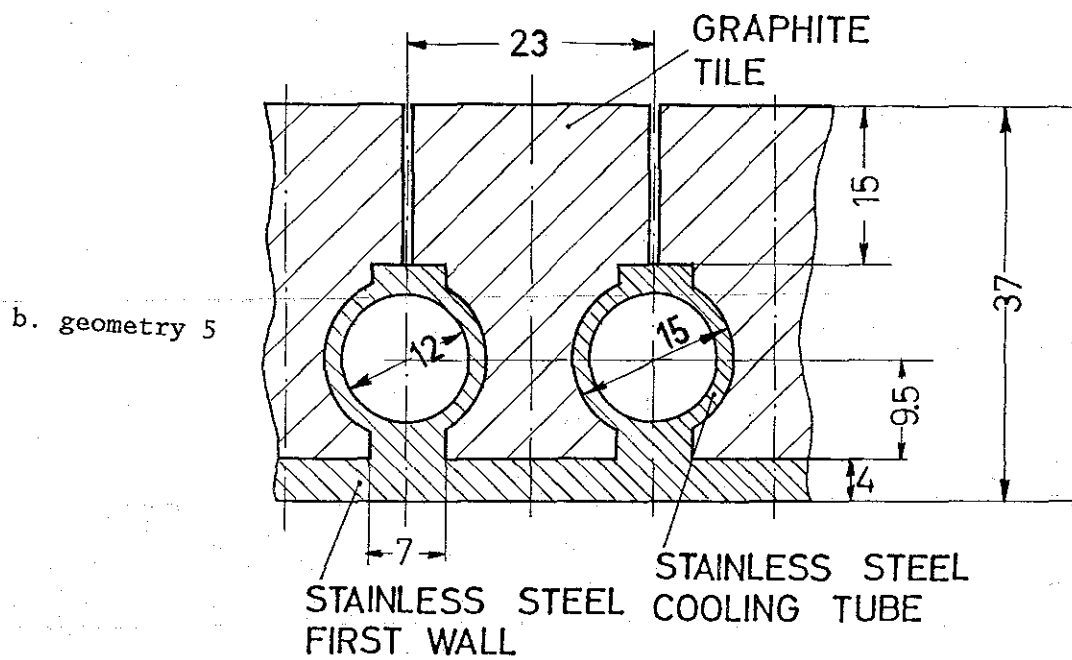
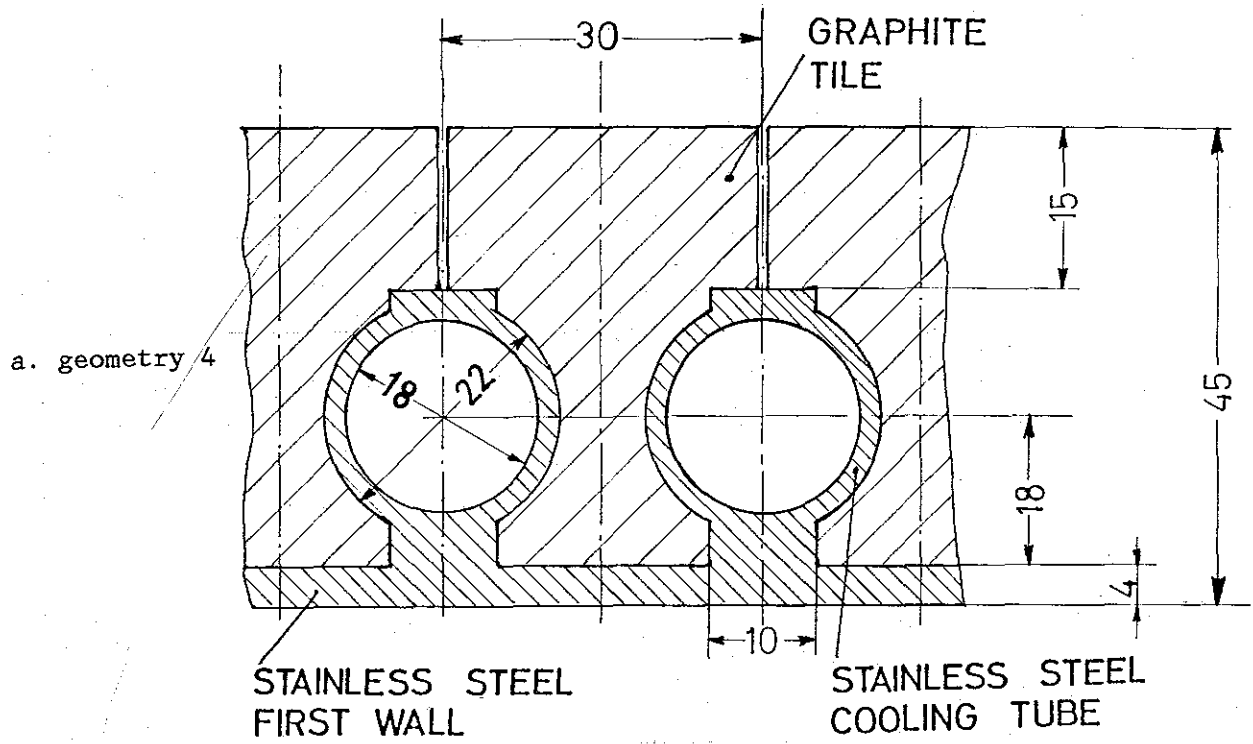


Figure 4. First wall designs with the tubes welded outside the canisters (dimensions in millimeters).

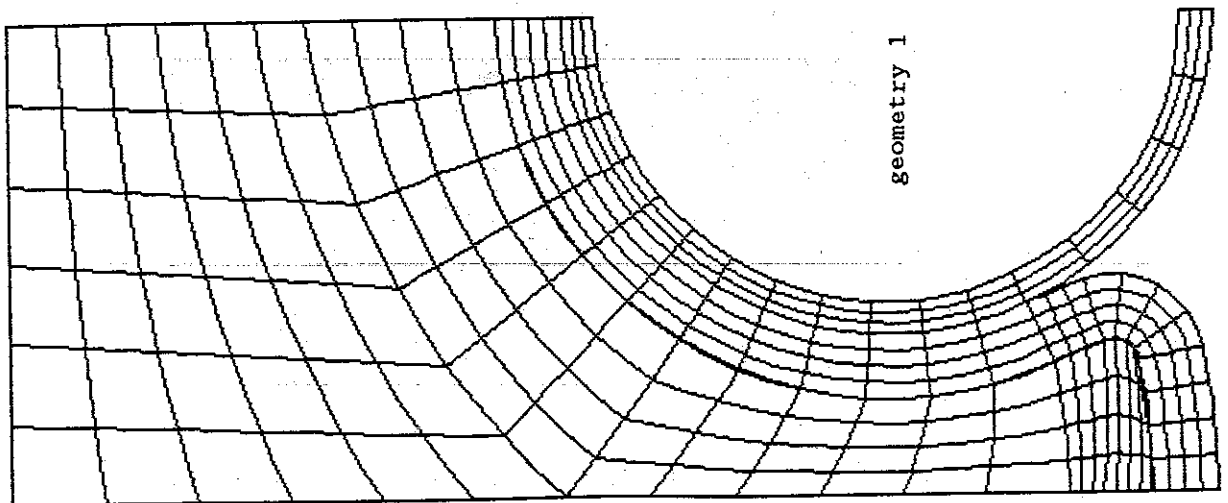
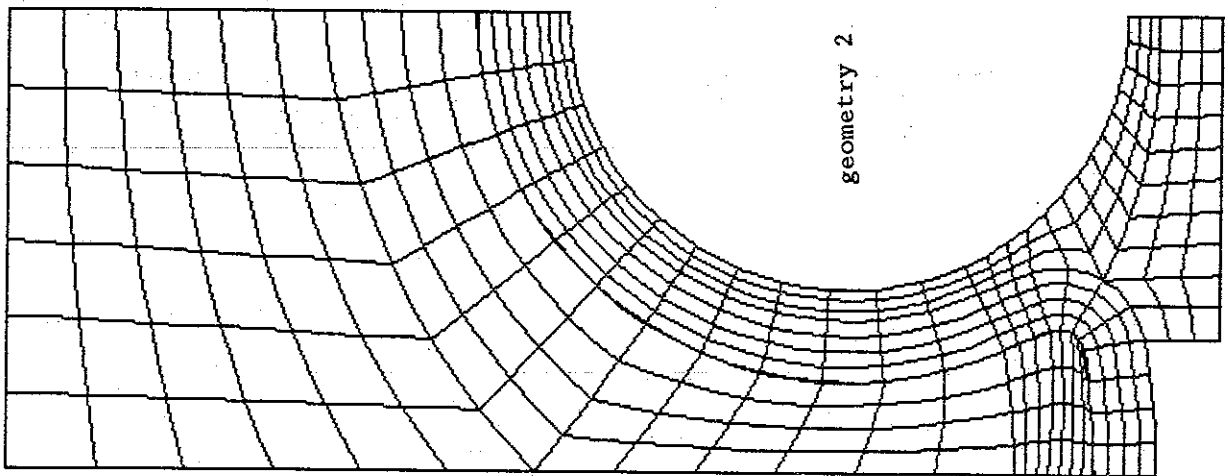
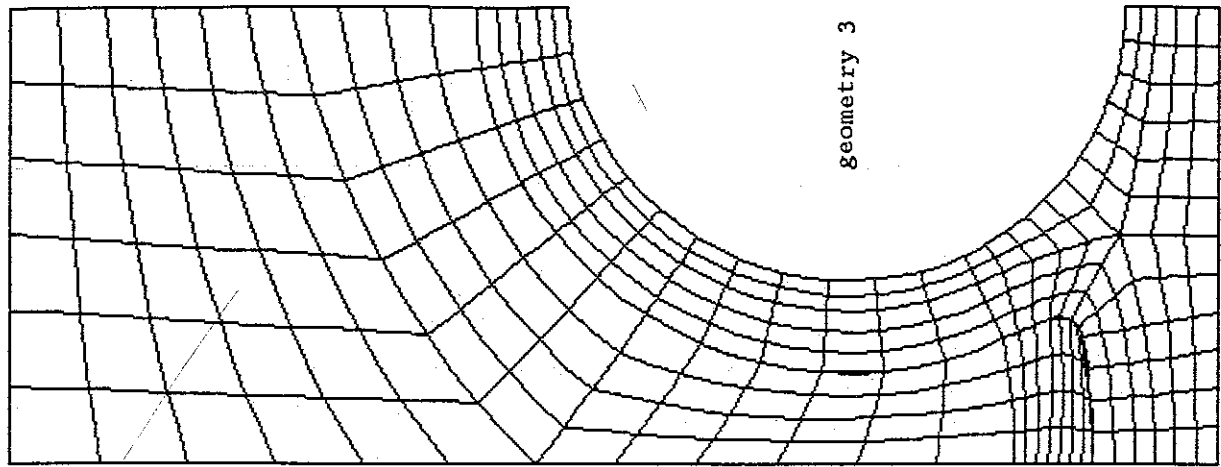


Figure 5. Mesh schematization for the geometries 1, 2 and 3.

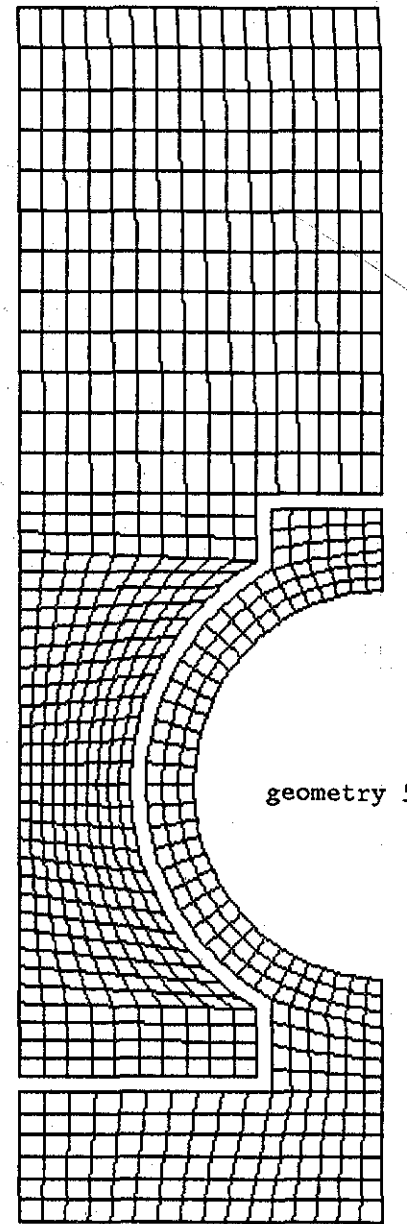
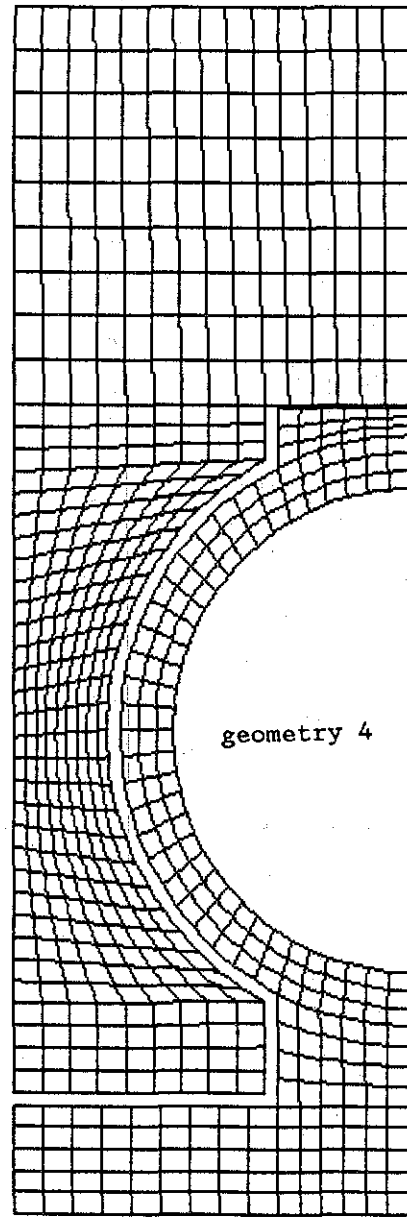


Figure 6. Mesh schematization for the geometries 4 and 5.

CALCULATION 1.

geometry 1

$\downarrow \dot{q}'' = 10. \text{ W/cm}^2$

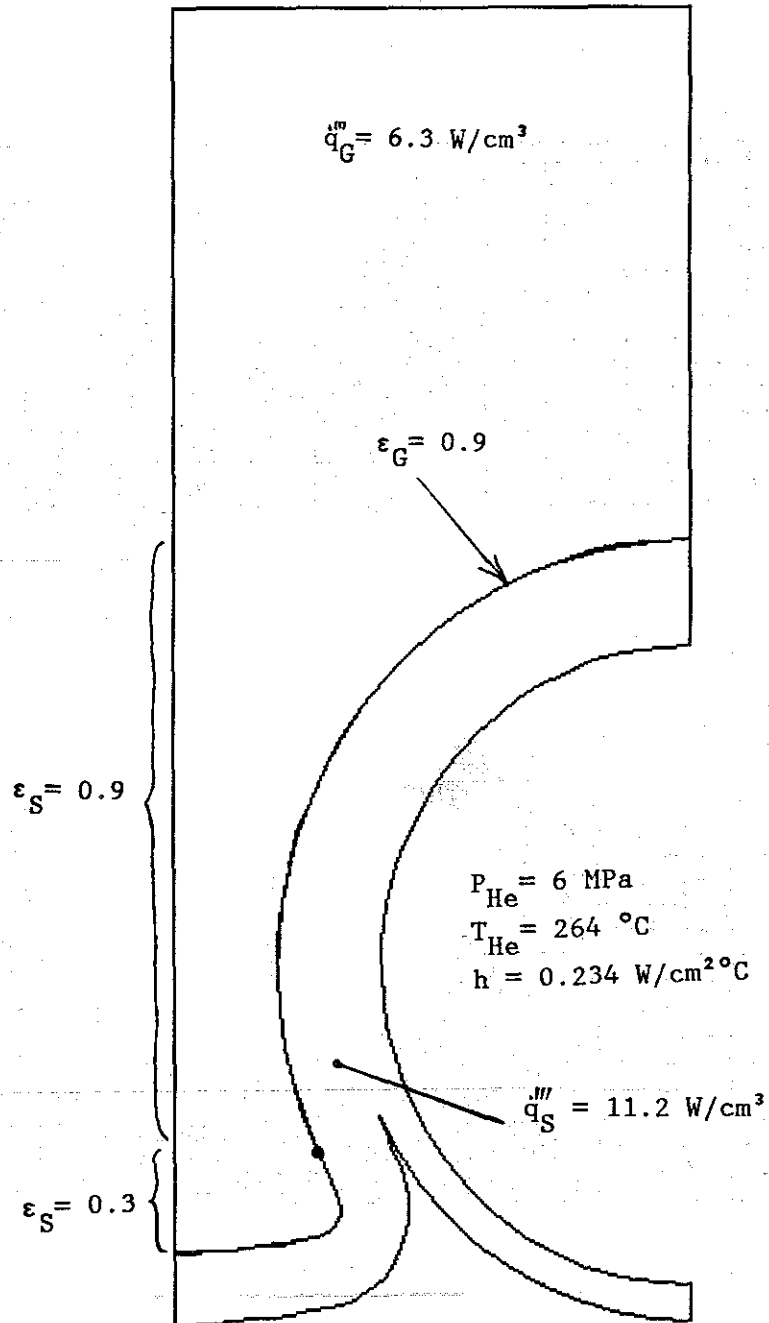
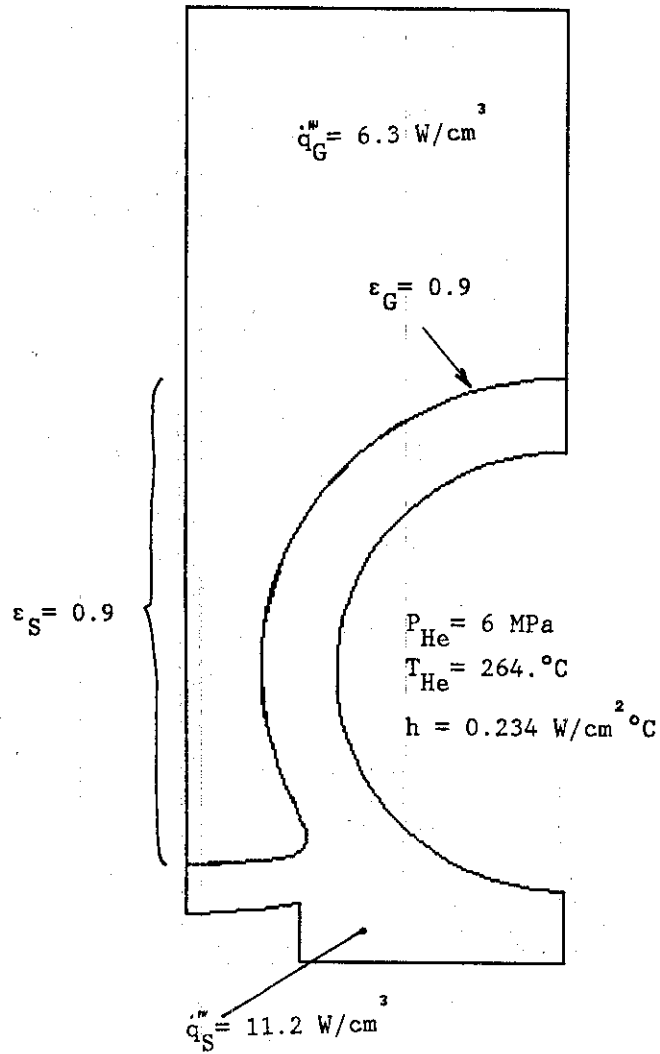


Figure 7. Boundary conditions for the calculation model 1

CALCULATION 2.1

geometry 2

$\dot{q}'' = 40. \text{ W/cm}^2$



CALCULATION 2.2

geometry 2

$\dot{q}'' = 40. \text{ W/cm}^2$

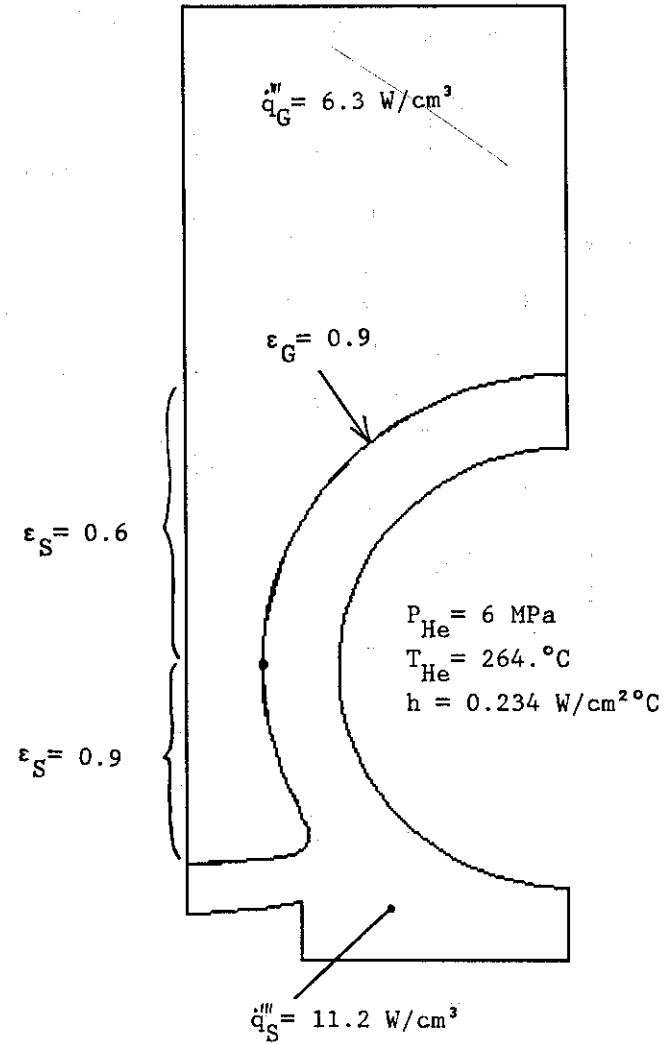
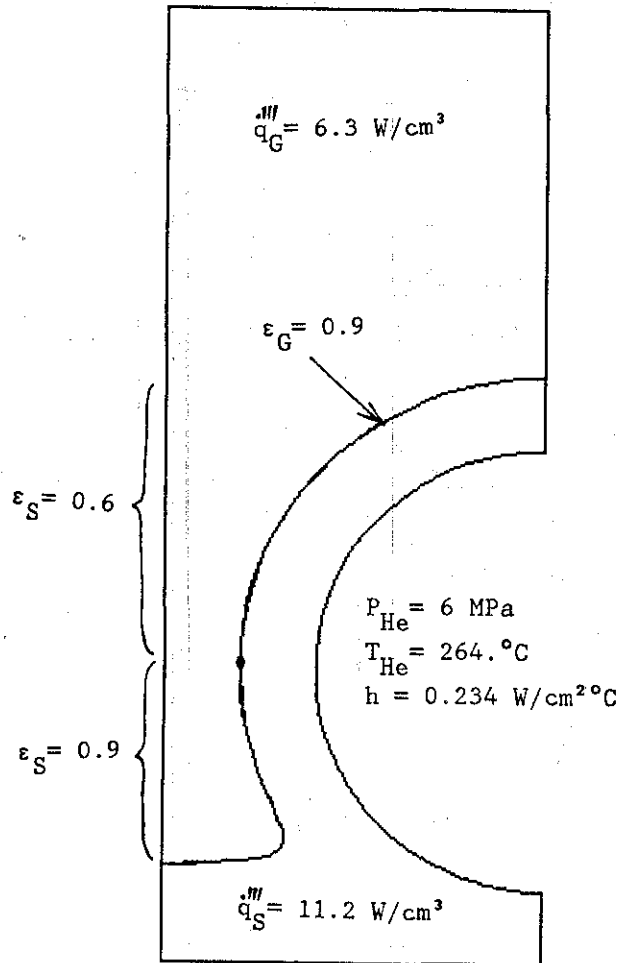


Figure 8. Boundary conditions for the calculation models 2.1 and 2.2

CALCULATION 3.1
geometry 3

$$\dot{q}'' = 40. \text{ W/cm}^2$$



CALCULATION 3.2
geometry 3

$$\dot{q}'' = 40. \text{ W/cm}^2$$

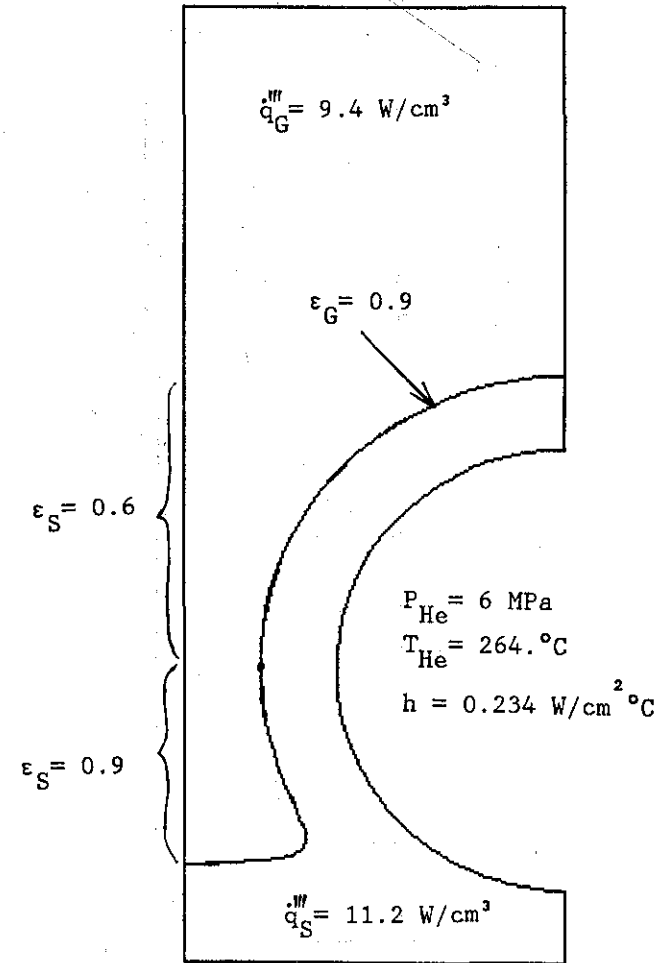
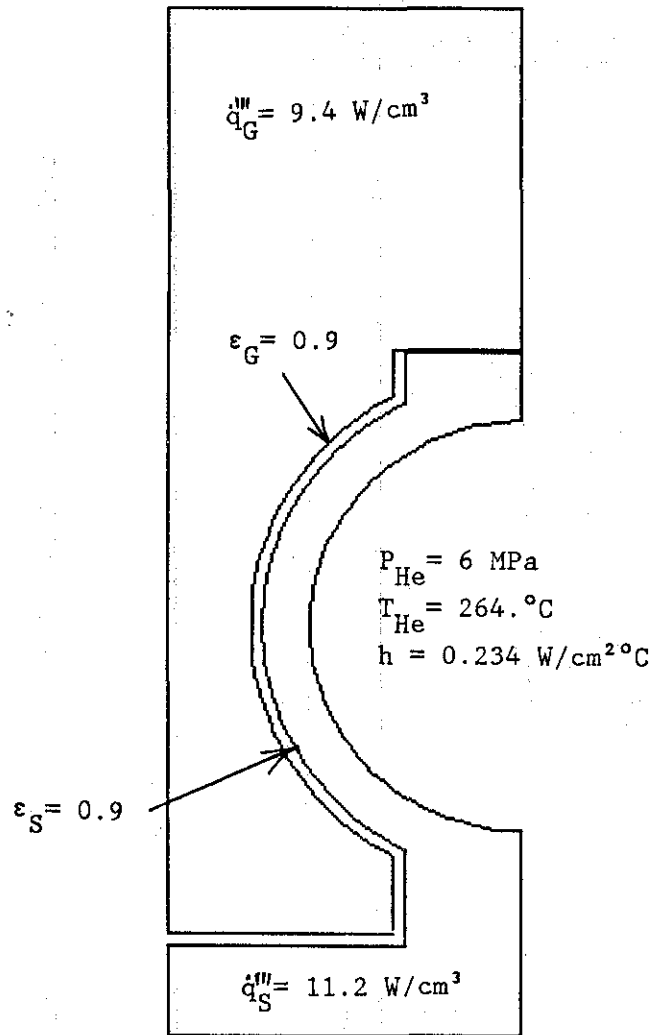


Figure 9. Boundary conditions for the calculation models 3.1 and 3.2

CALCULATION 4.

geometry 4

$\downarrow \dot{q}'' = 20. \text{ W/cm}^2$



CALCULATION 5.

geometry 5

$\downarrow \dot{q}'' = 40. \text{ W/cm}^2$

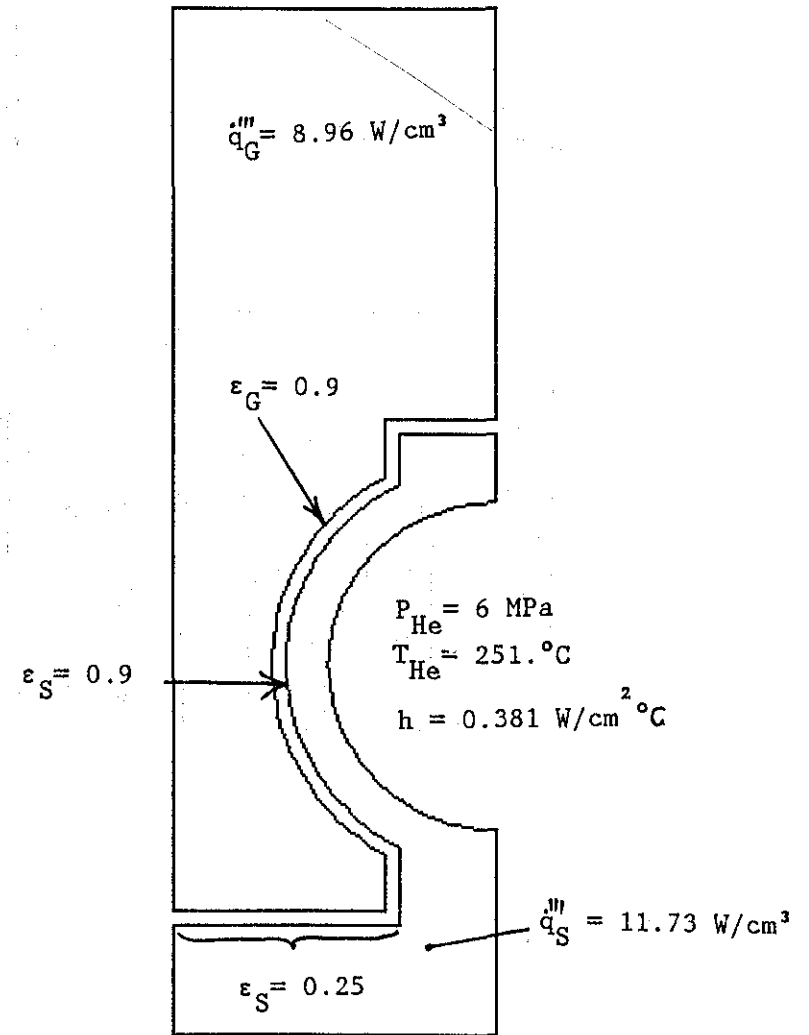


Figure 10. Boundary conditions for the calculation models 4. and 5.

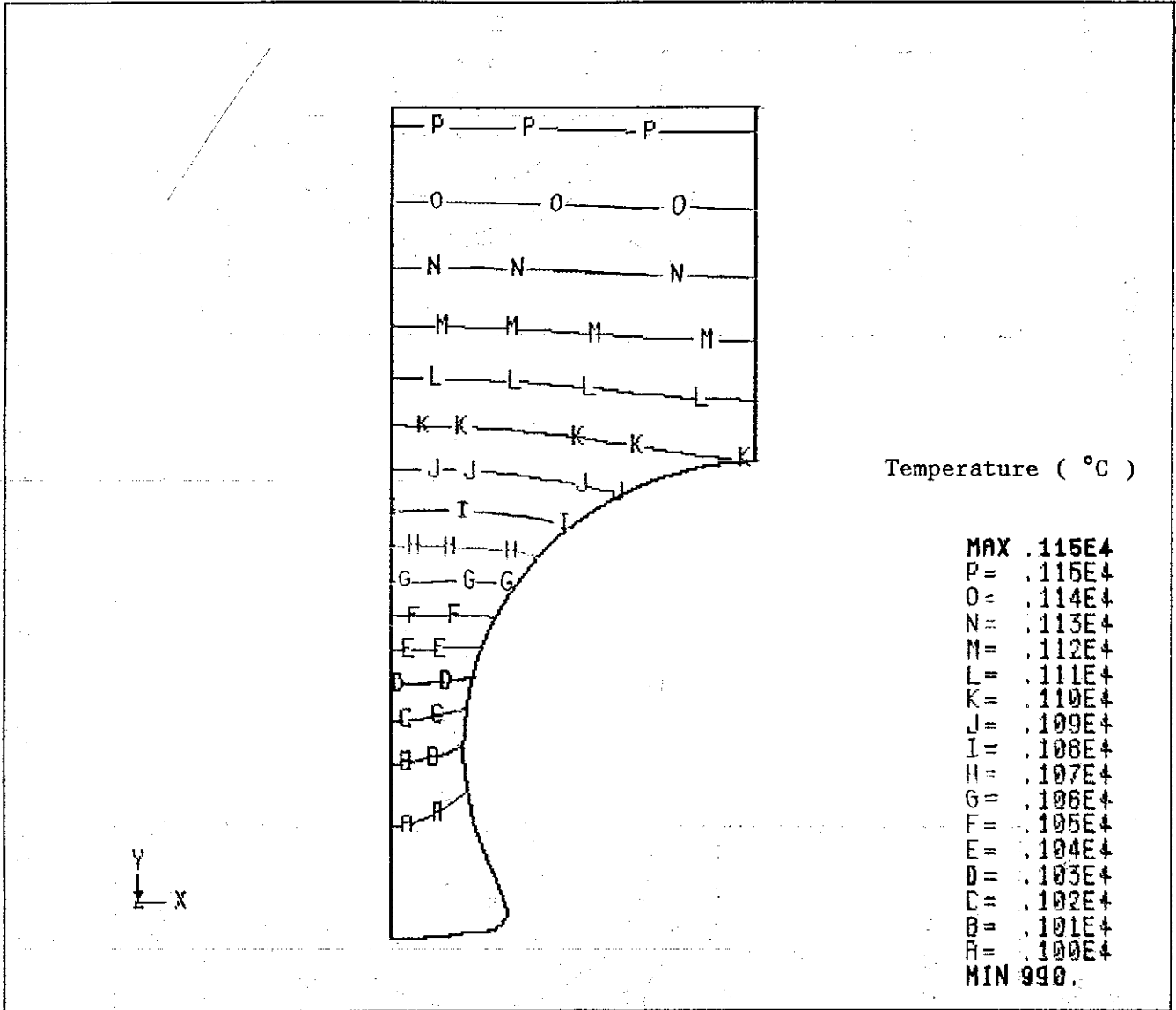


Figure 11. Temperature contours in tile for the calculation 1.

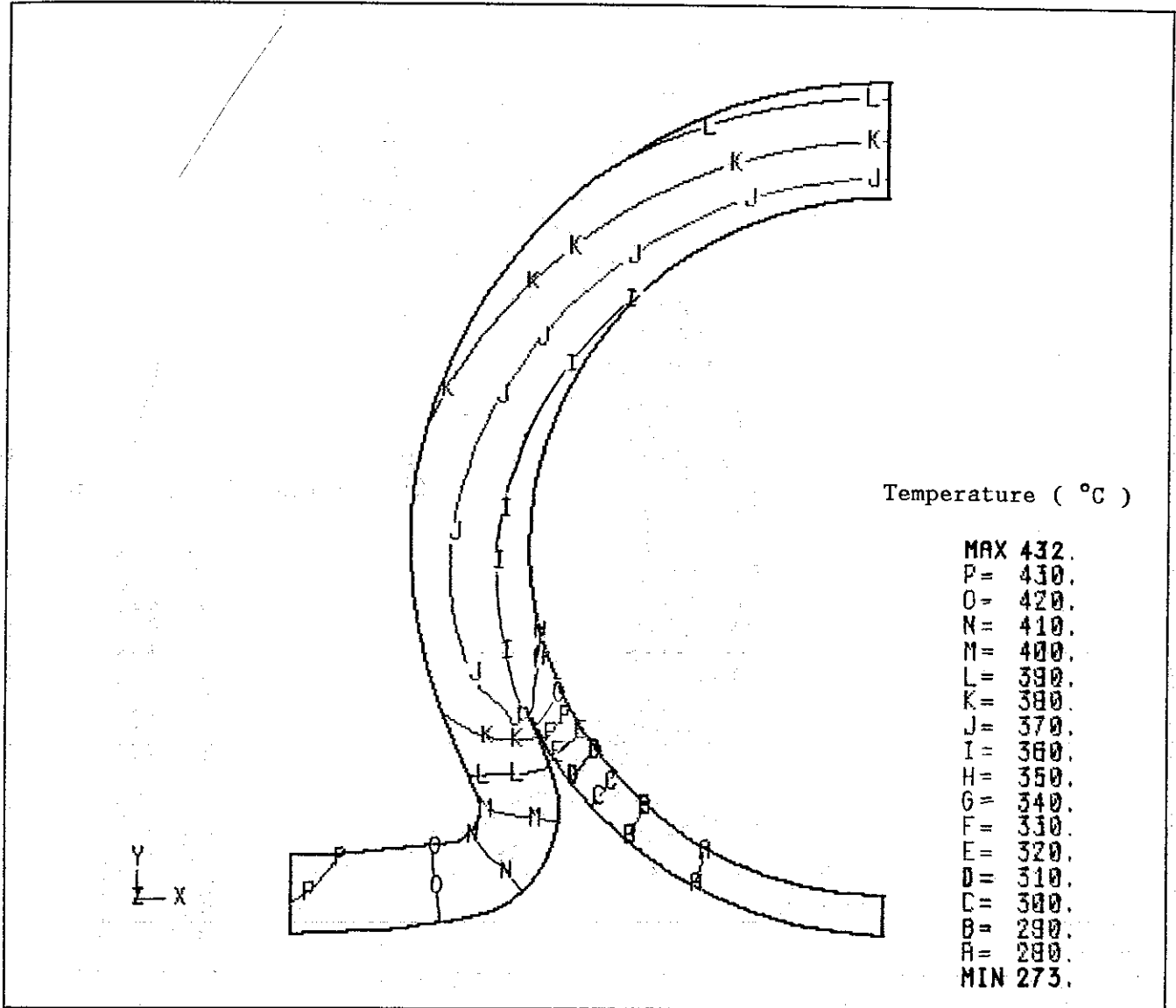


Figure 12. Temperature contours in steel for the calculation 1.

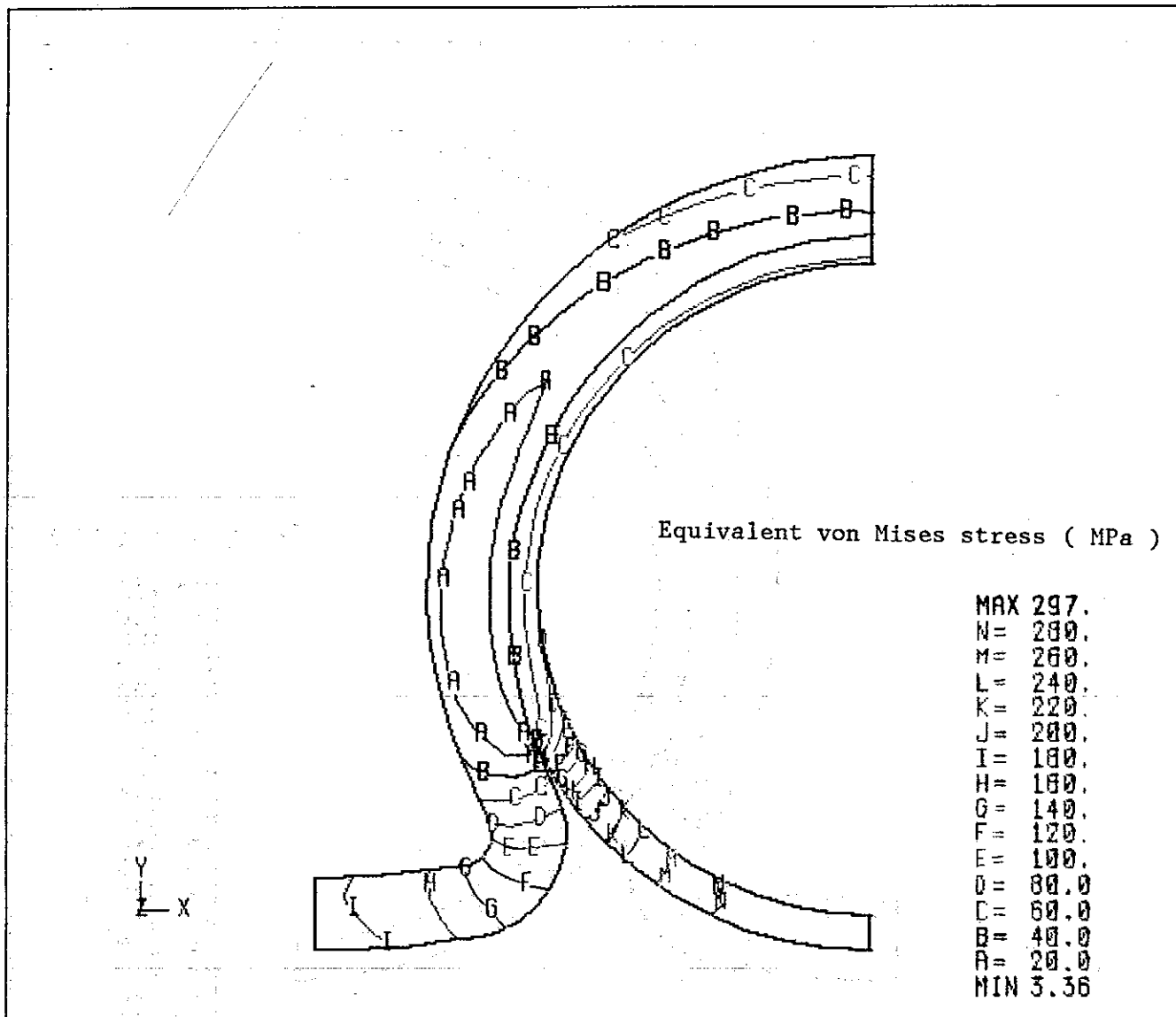


Figure 13. Equivalent von Mises stress contours in steel for the calculation 1.

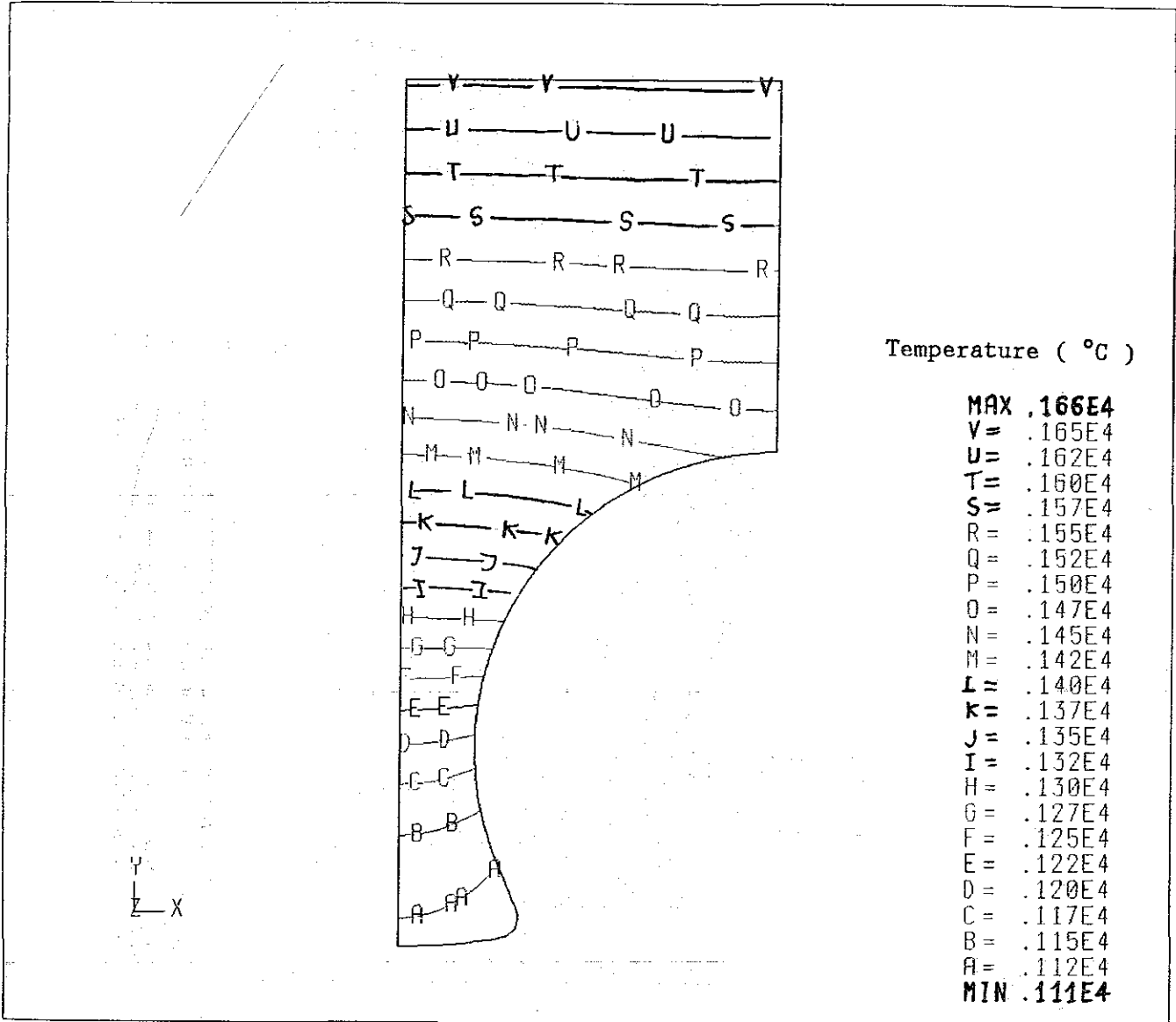


Figure 14. Temperature contours in tile for the calculation 2.1

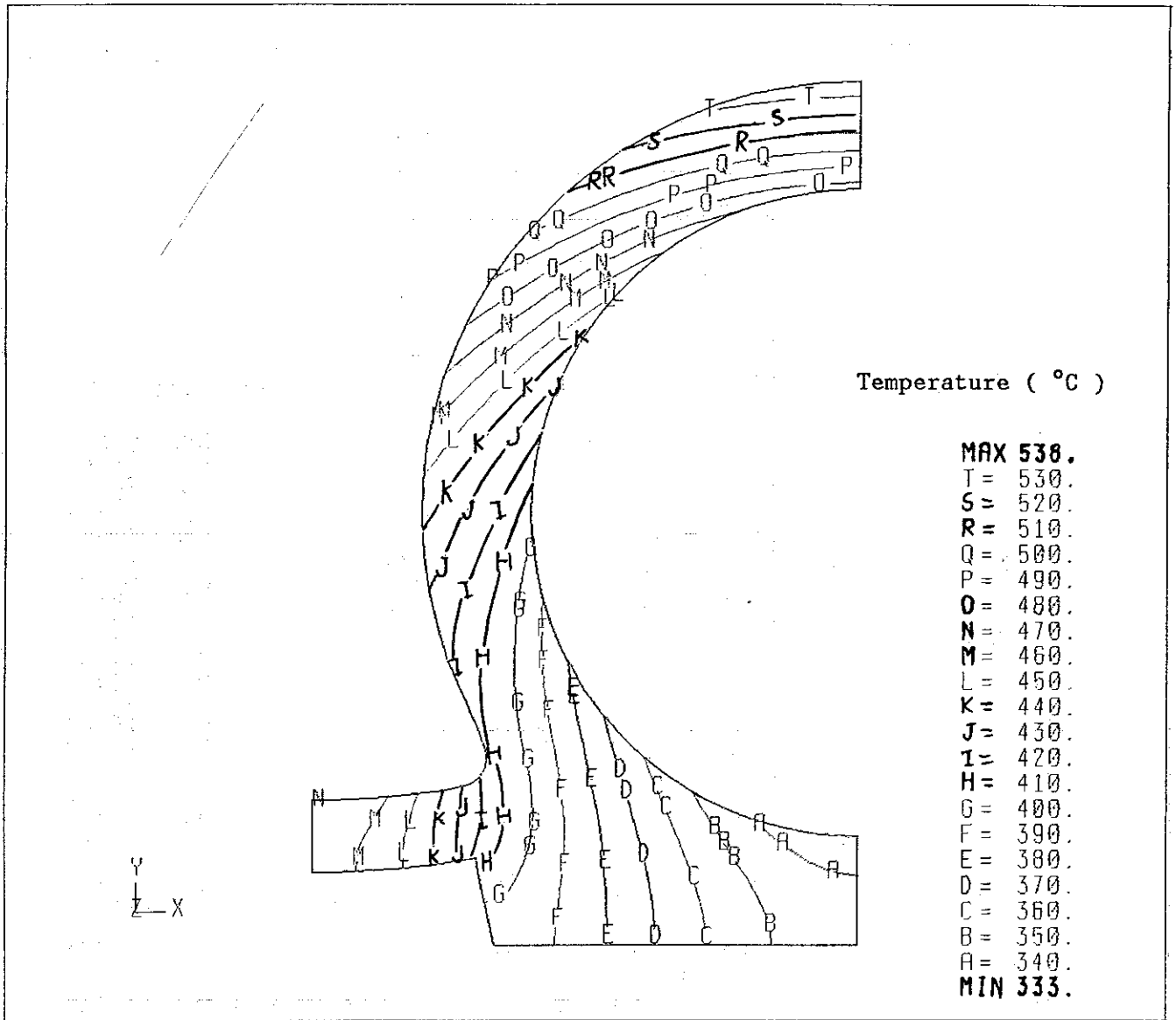


Figure 15. Temperature contours in steel for the calculation 2.1

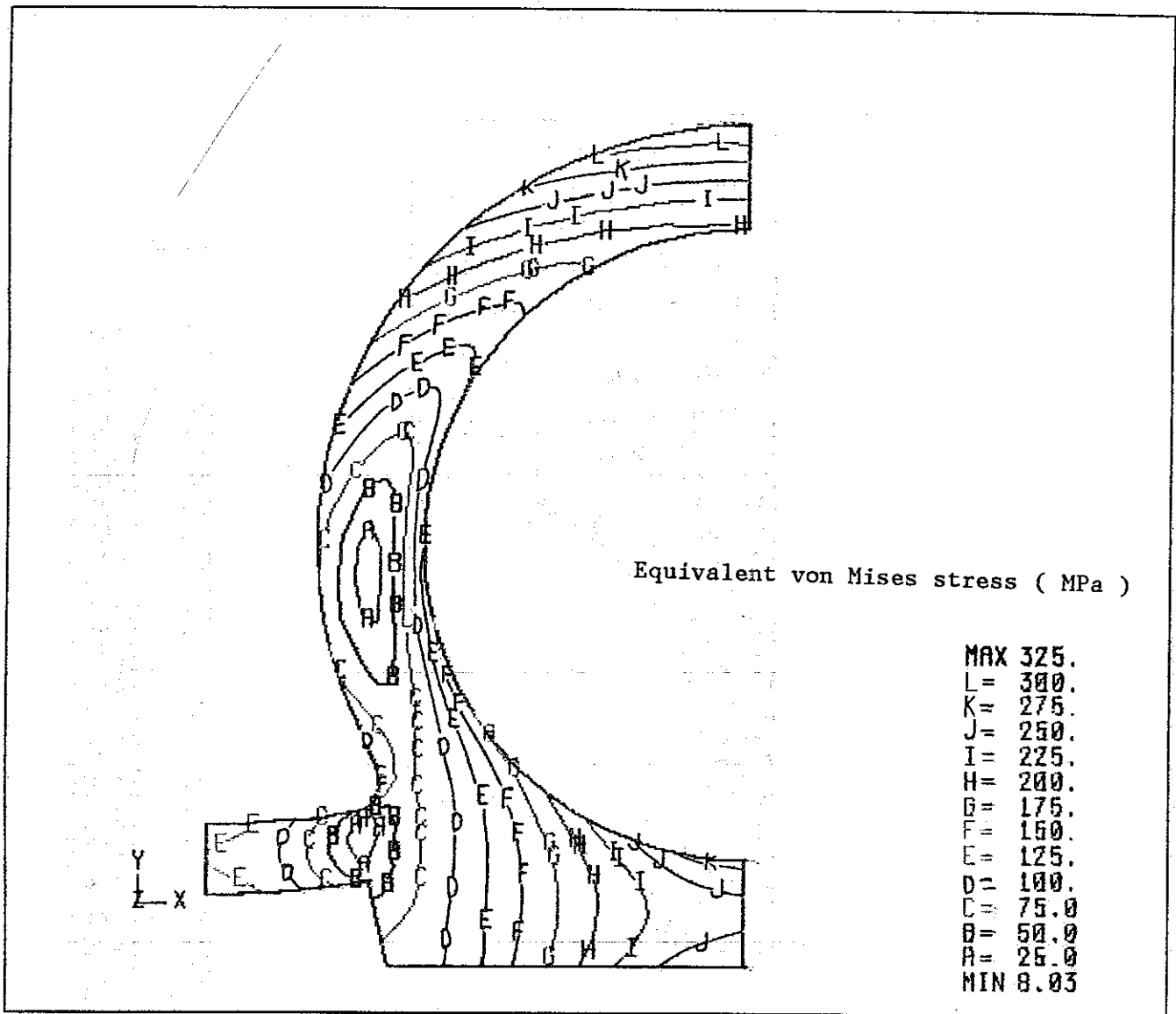


Figure 16. Equivalent von Mises stress contours in steel for the calculation 2.1.

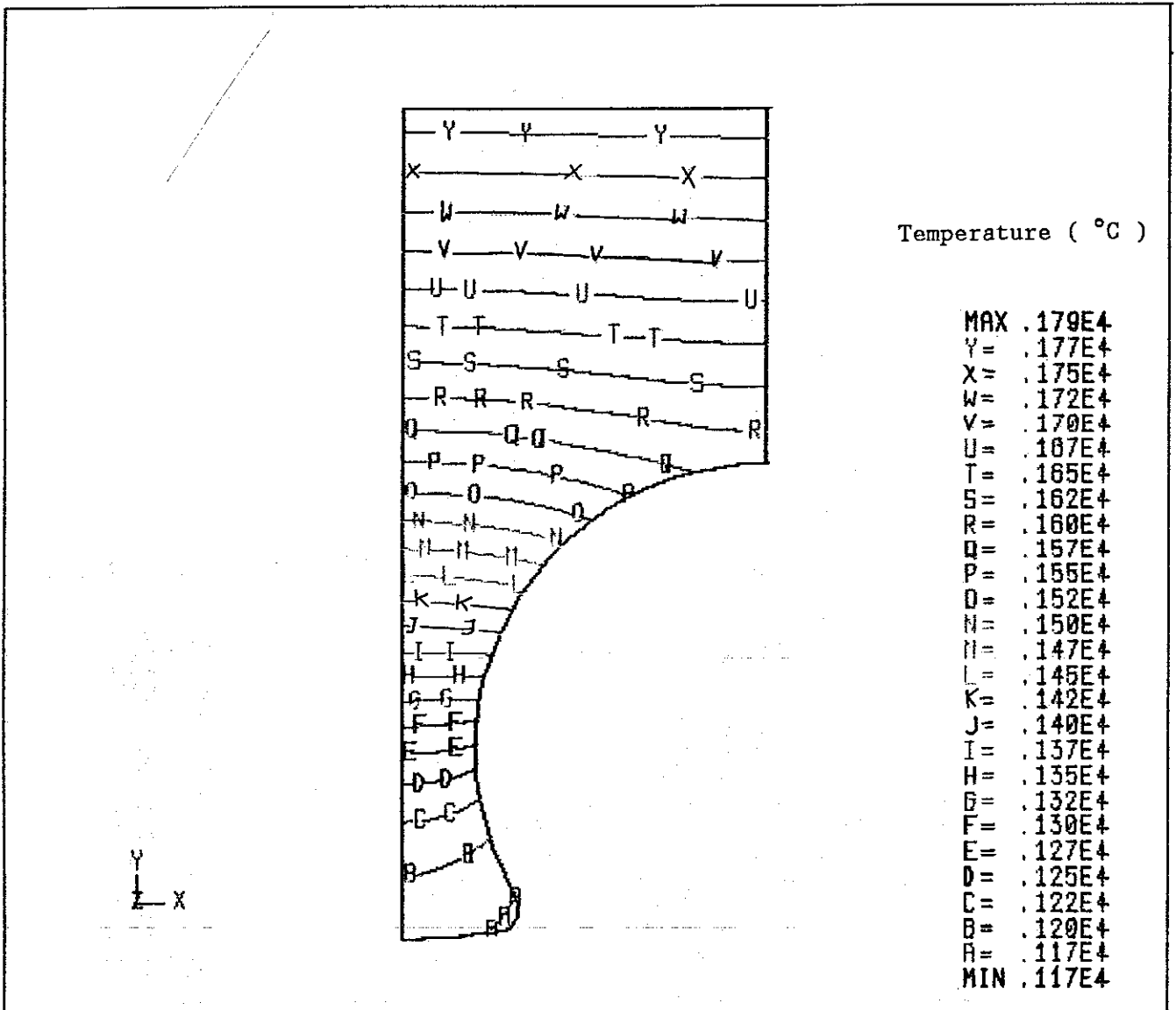


Figure 17. Temperature contours in tile for the calculation 2.2

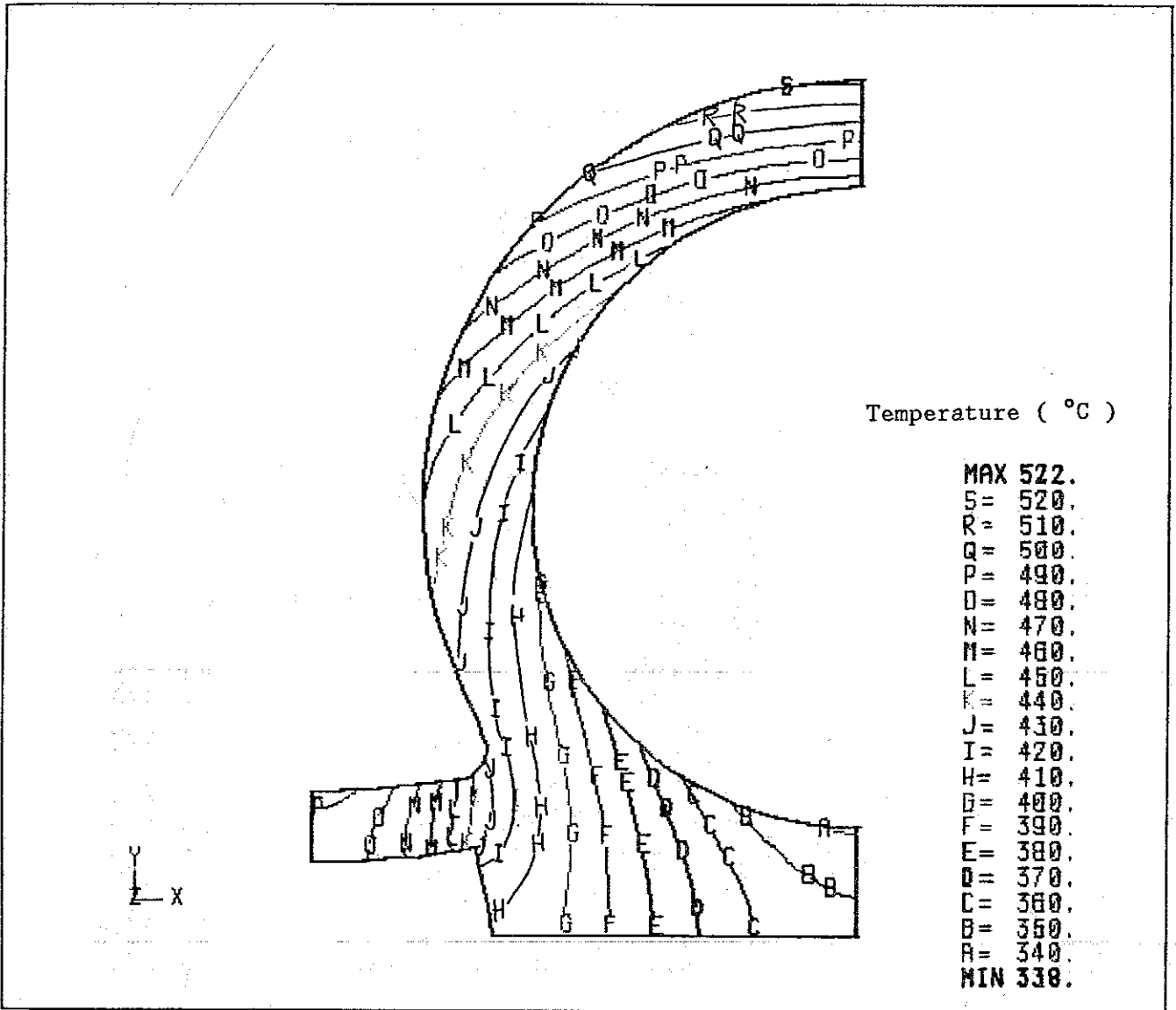


Figure 18. Temperature contours in steel for the calculation 2.2

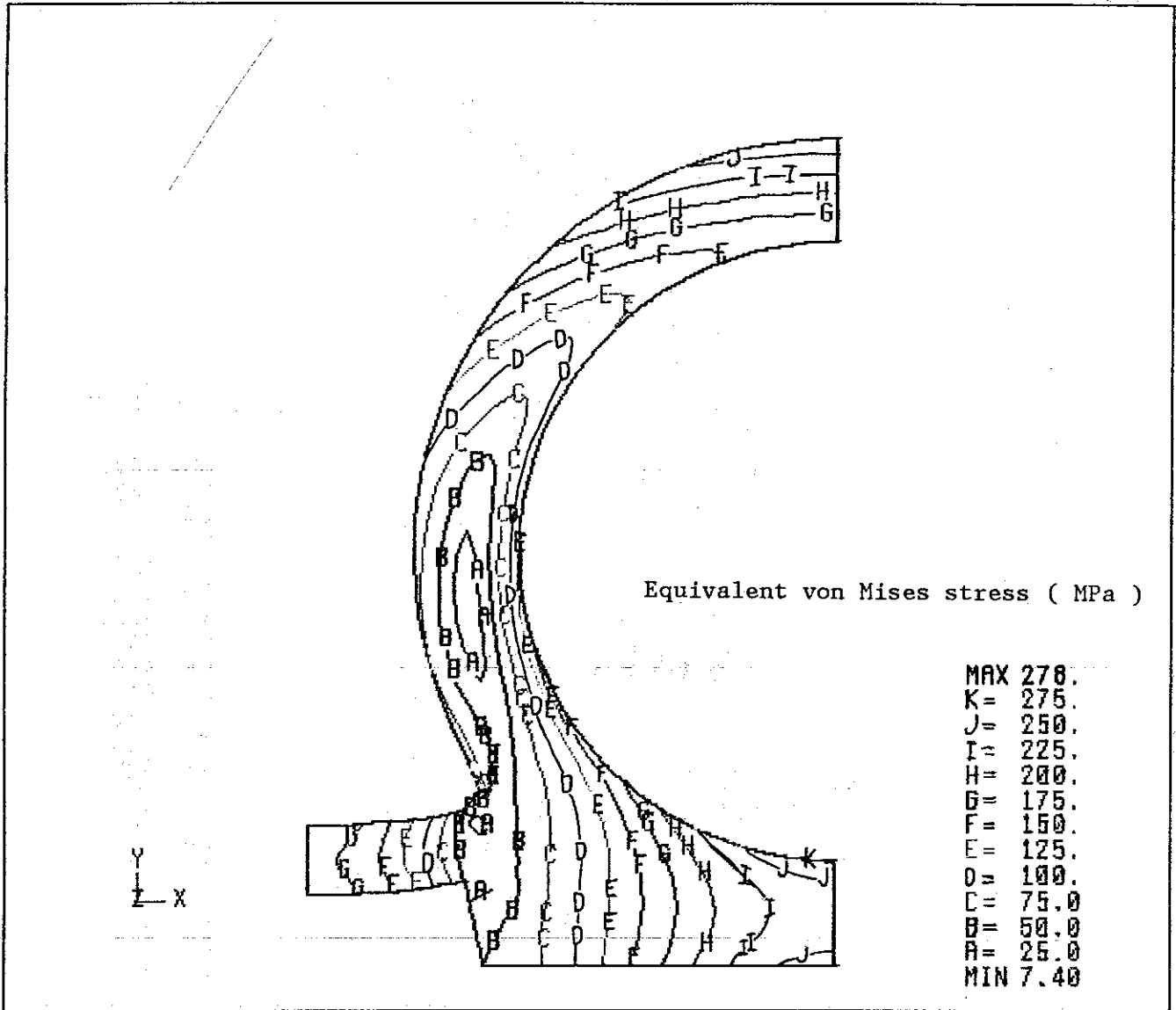


Figure 19. Equivalent von Mises stress contours in steel for the calculation 2.2

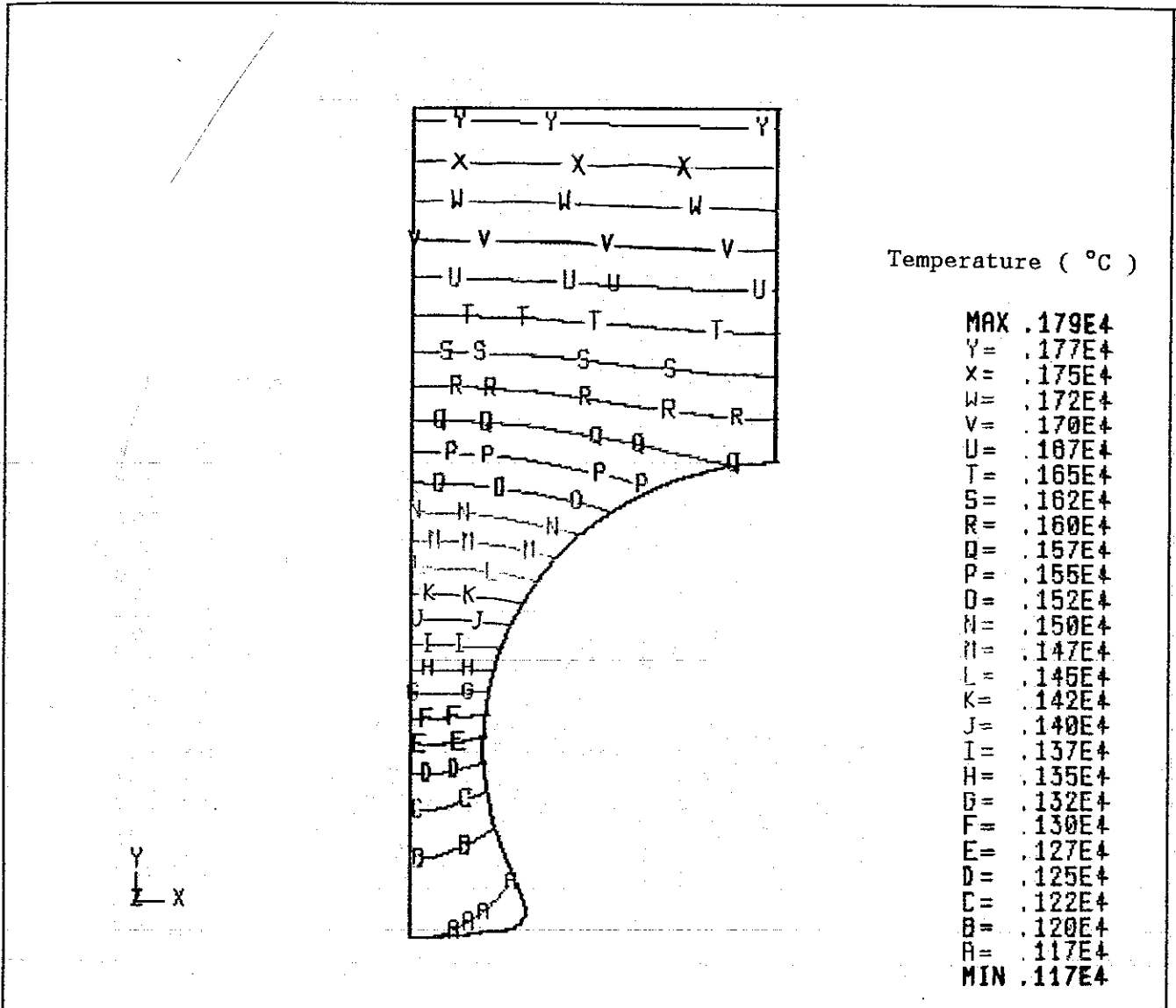


Figure 20. Temperature contours in tile for the calculation 3.1

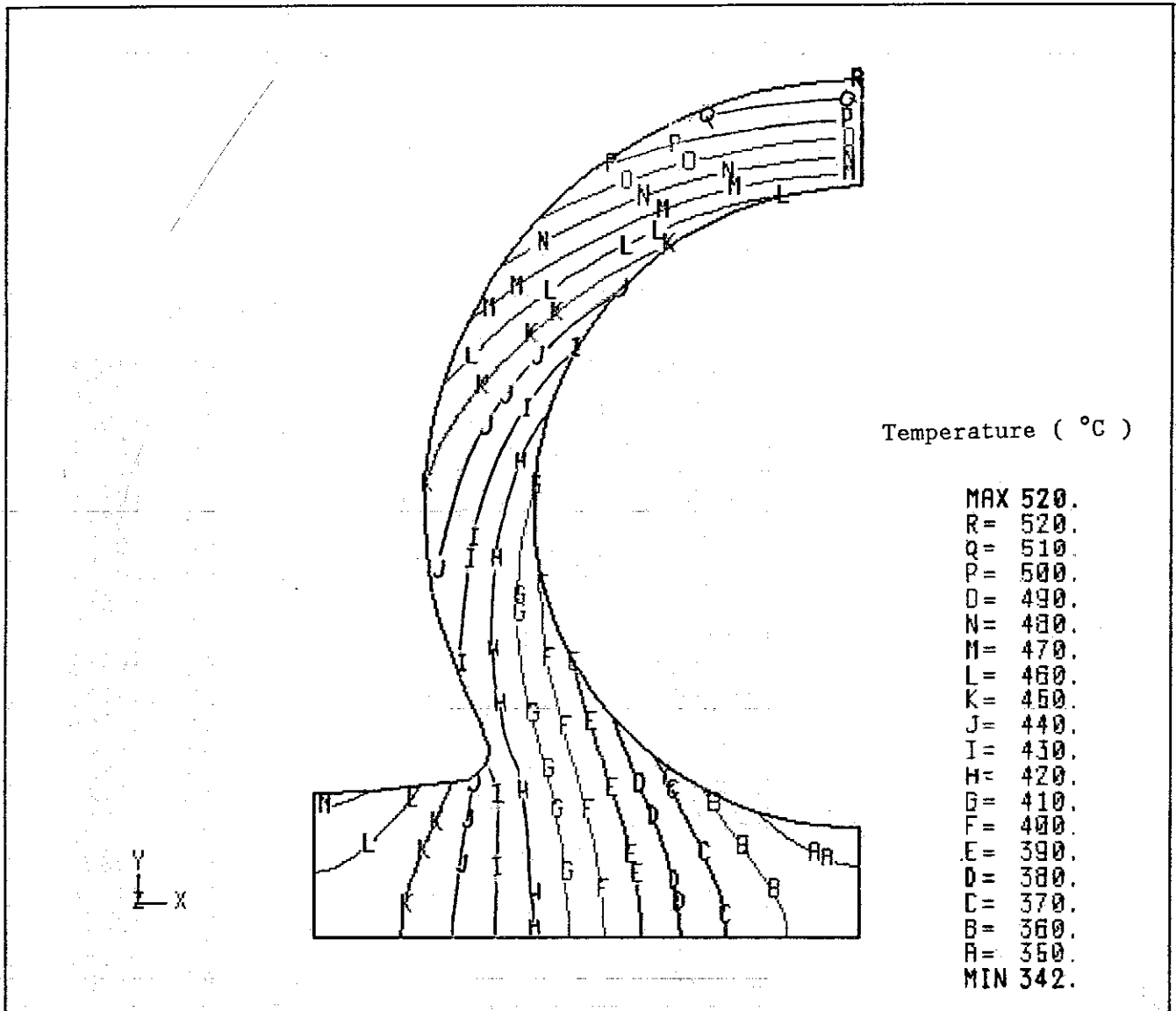


Figure 21. Temperature contours in steel for the calculation 3.1

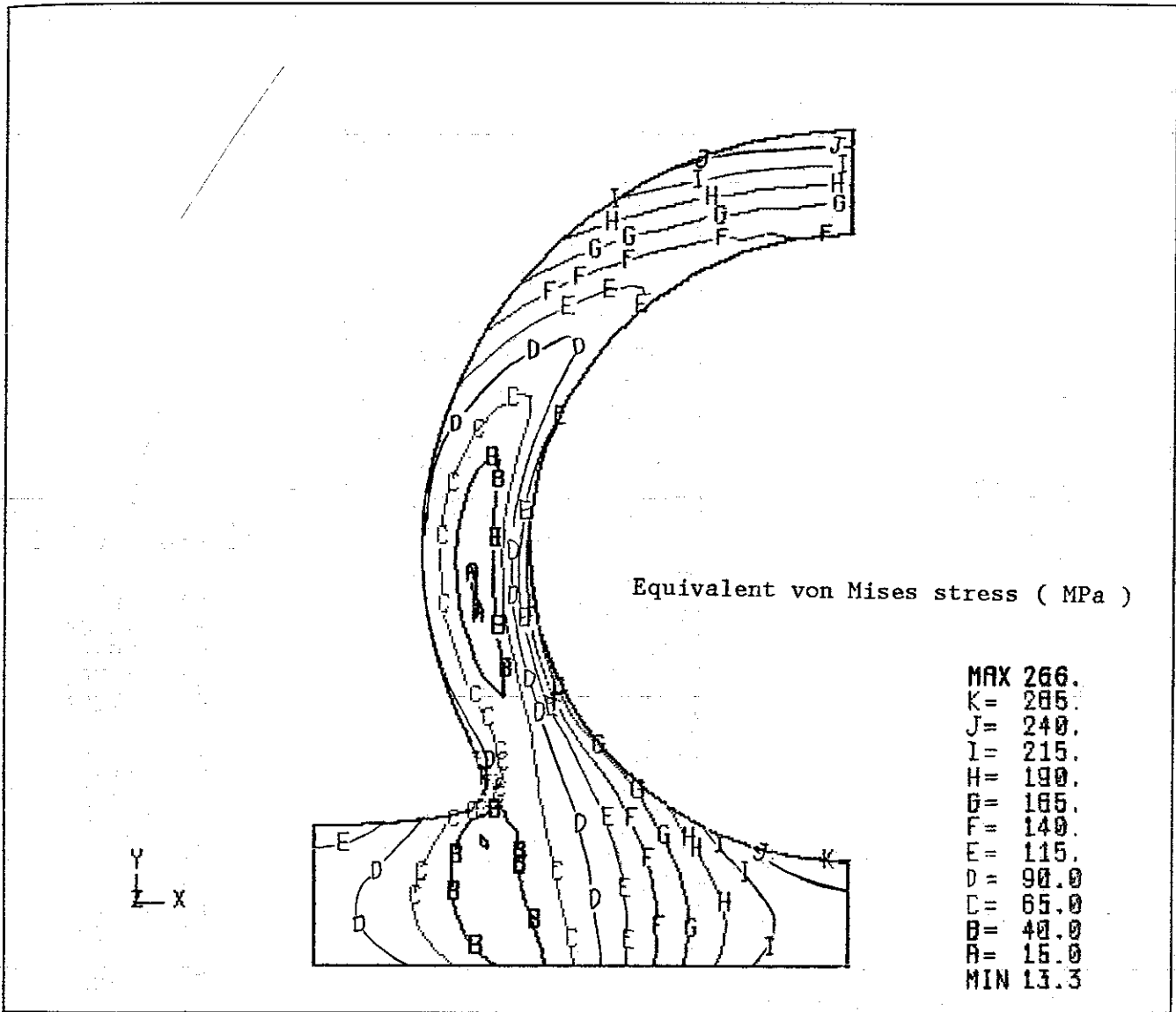


Figure 22. Equivalent von Mises stress contours in steel for the calculation 3.1

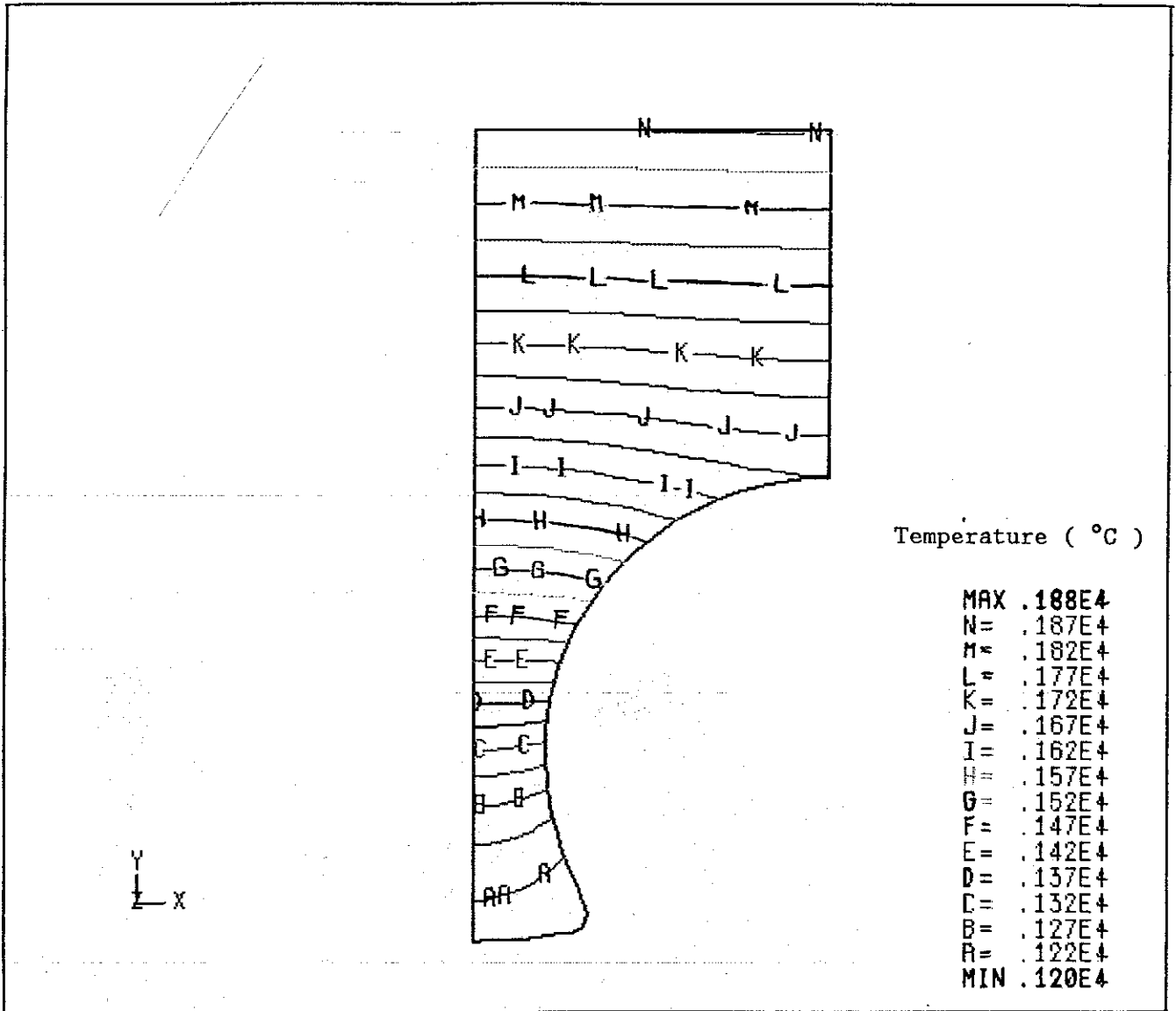


Figure 23. Temperature contours in tile for the calculation 3.2

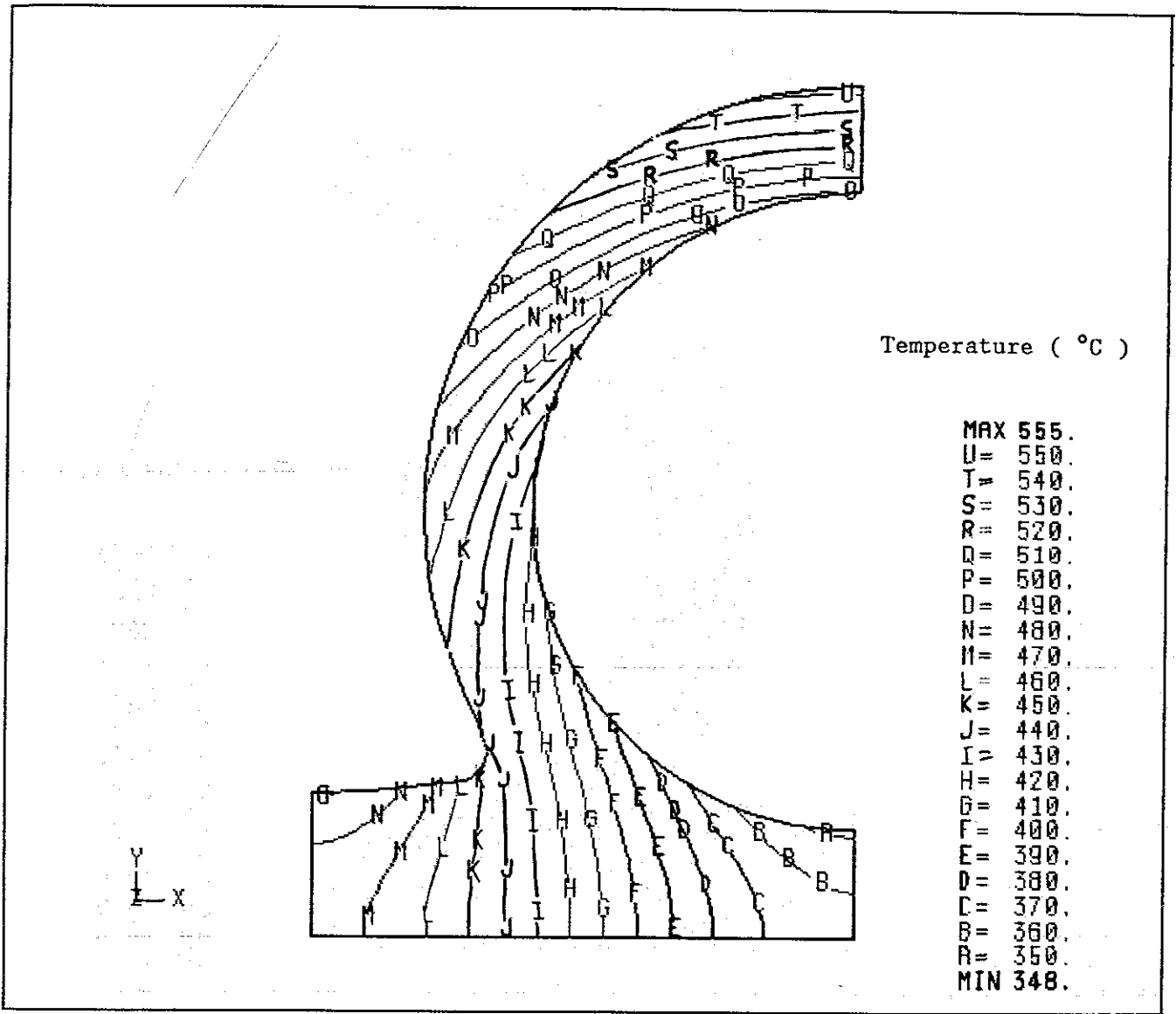


Figure 24. Temperature contours in steel for the calculation 3.2

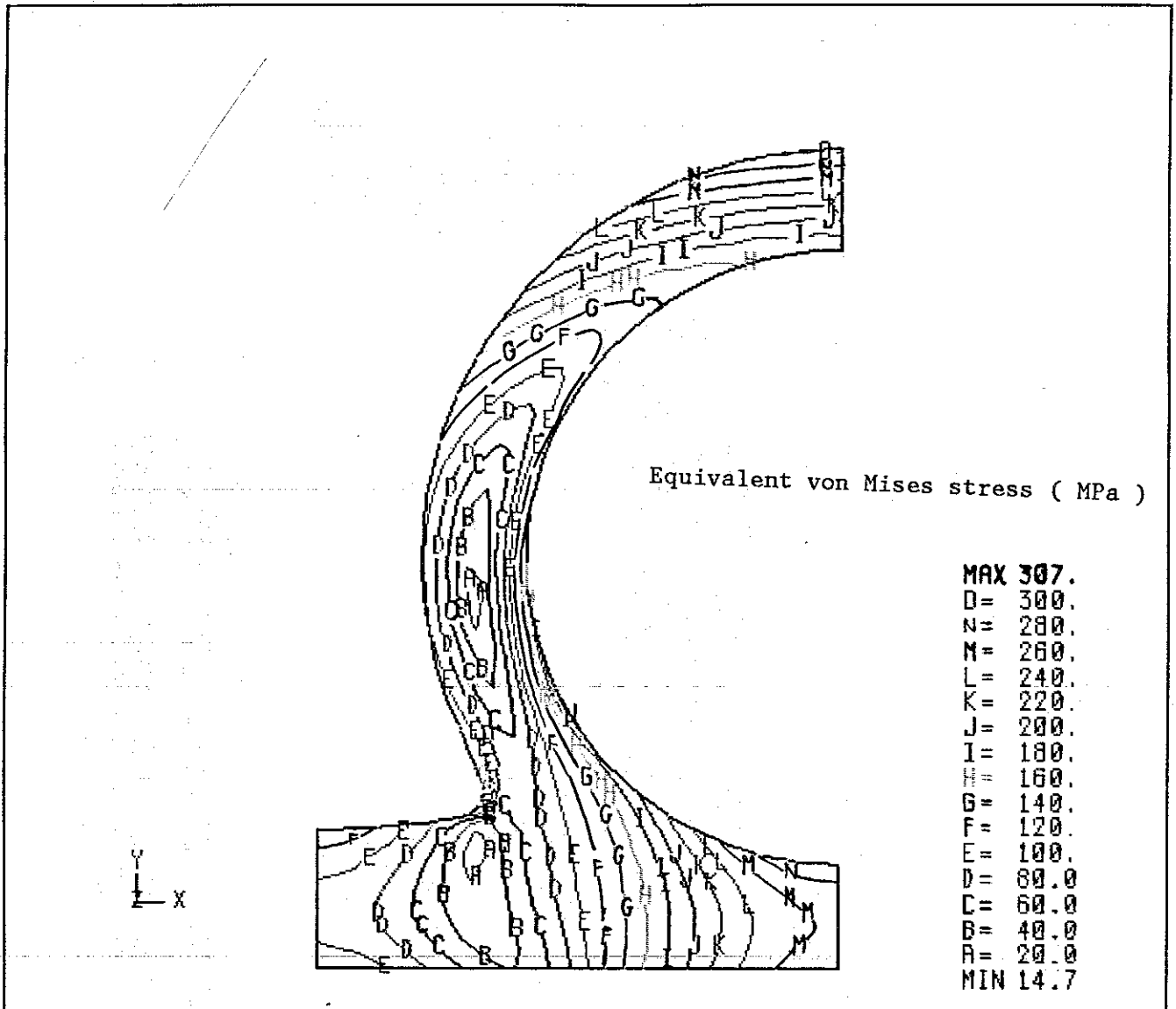


Figure 25. Equivalent von Mises stress contours in steel for the calculation 3.2

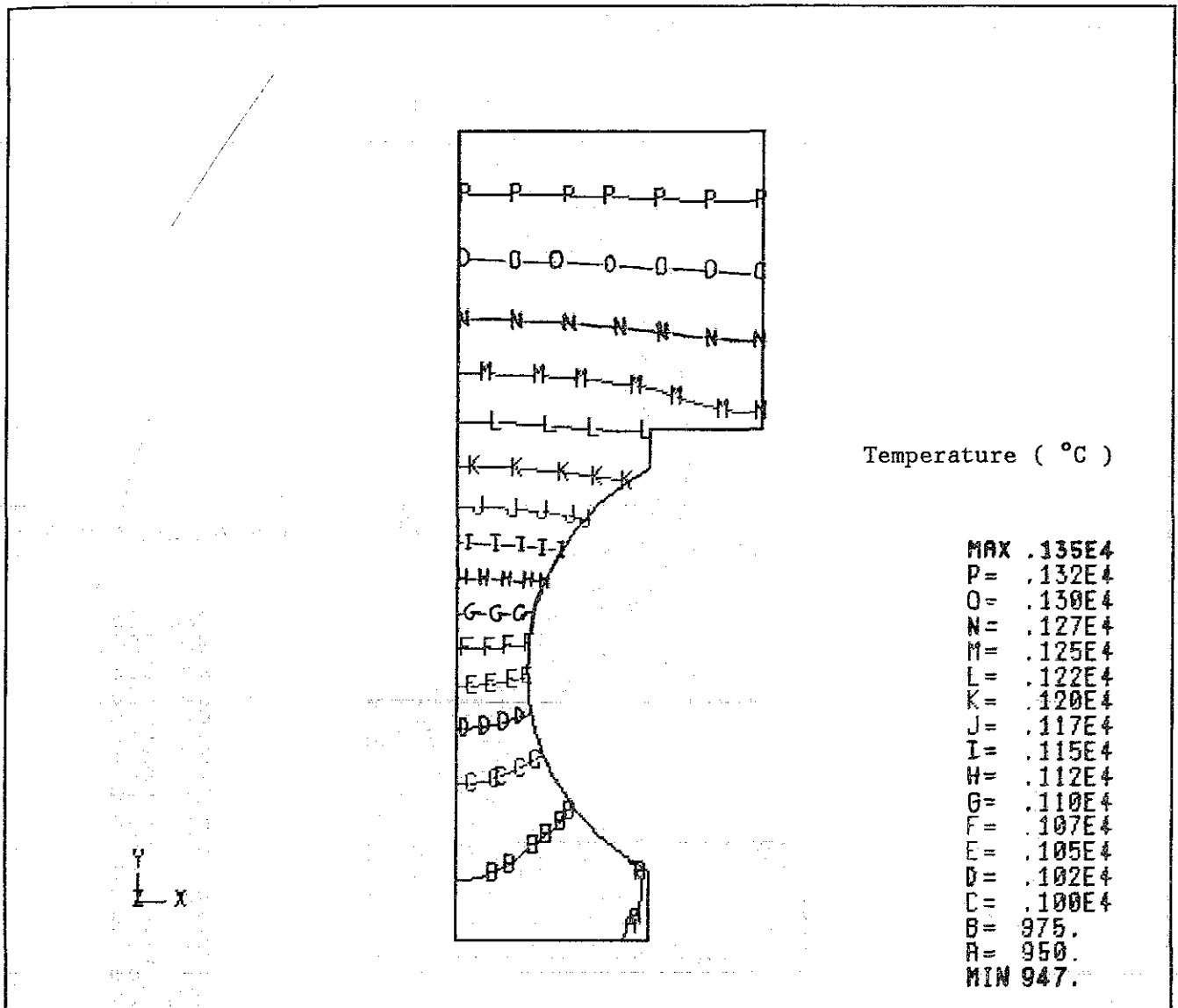


Figure 26. Temperature contours in tile for the calculation 4.

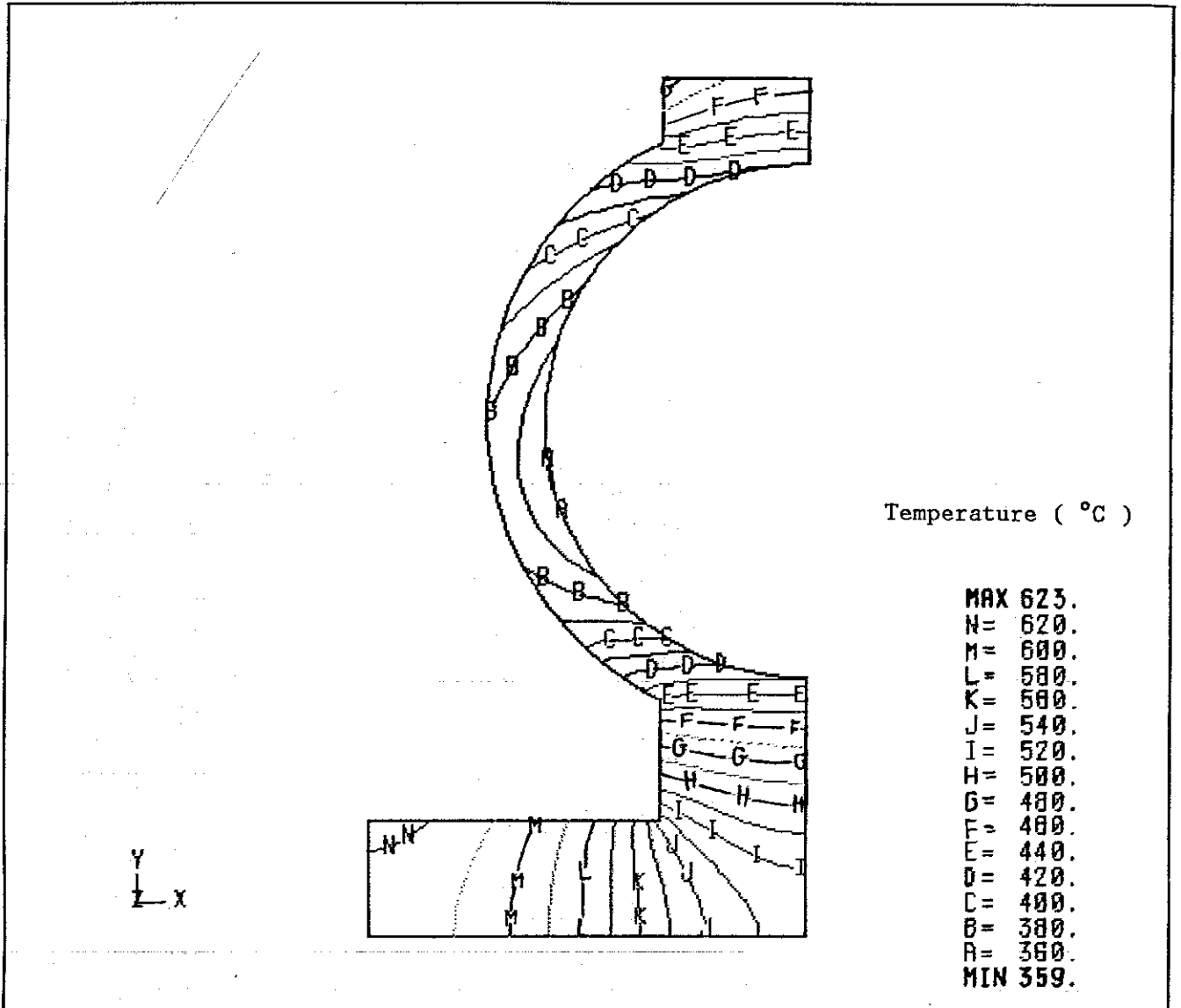


Figure 27. Temperature contours in steel for the calculation 4.

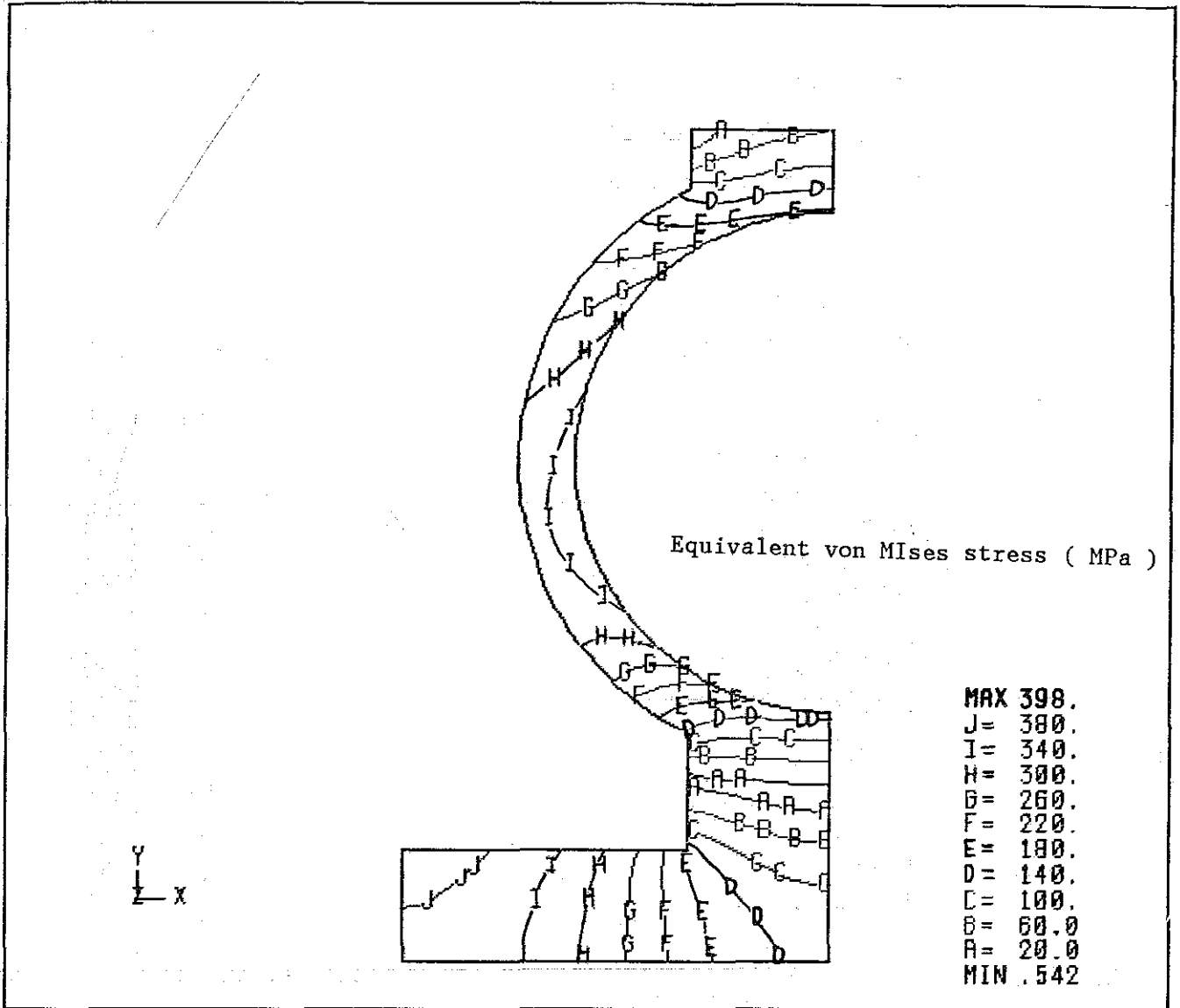


Figure 28. Equivalent von Mises stress contours in steel for the calculation 4.

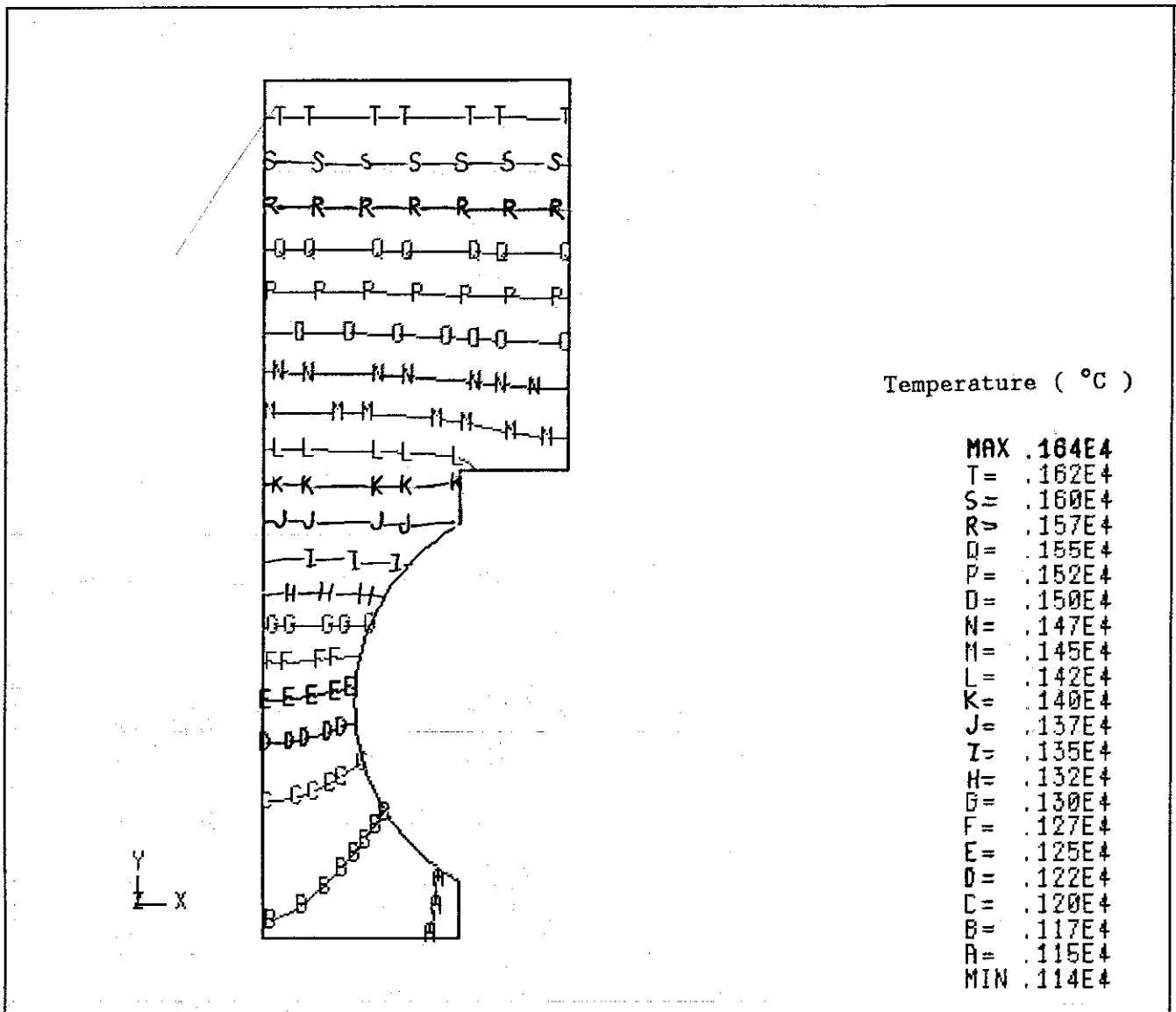


Figure 29. Temperature contours in tile for the calculation 5.

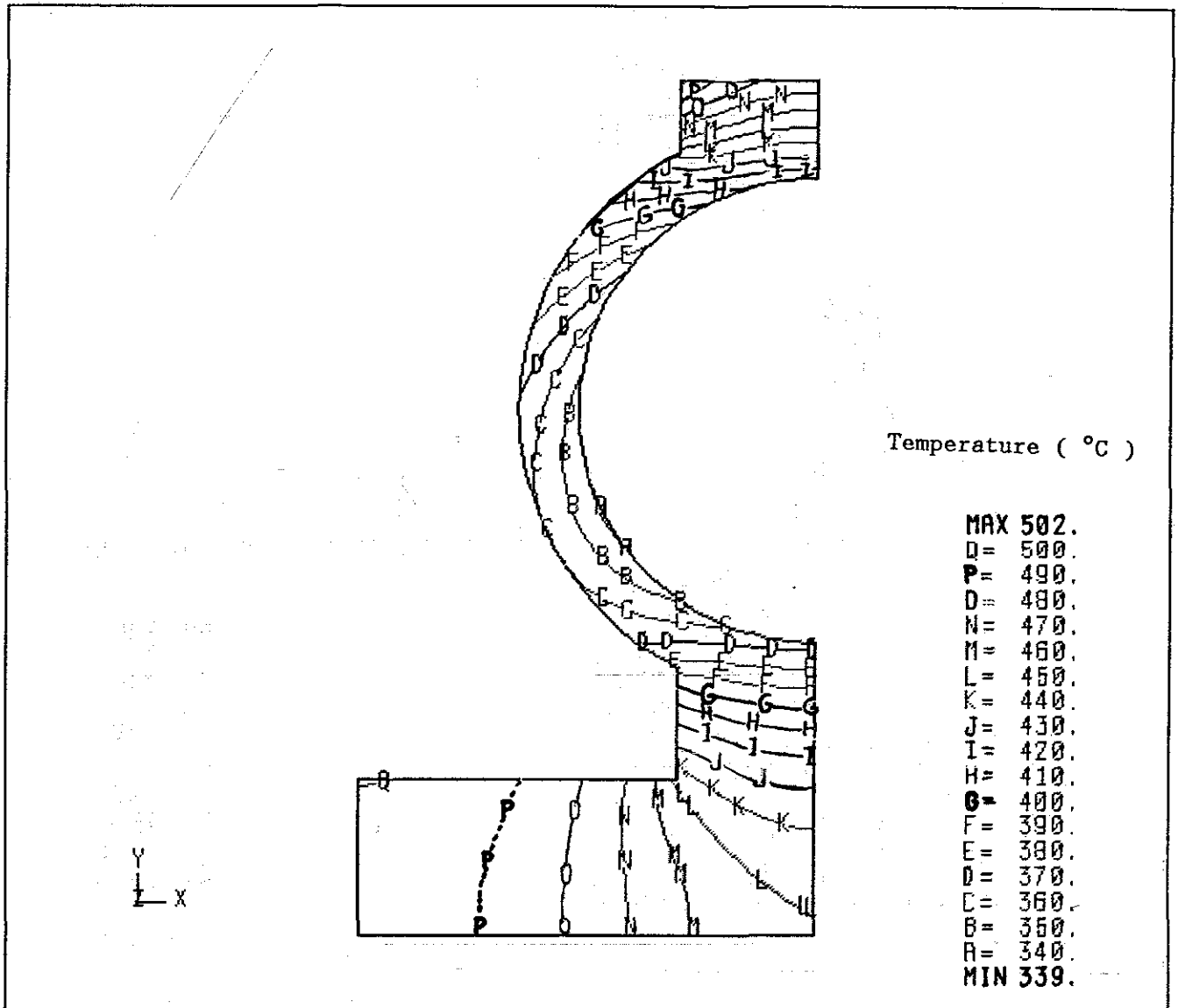


Figure 30. Temperature contours in steel for the calculation 5.

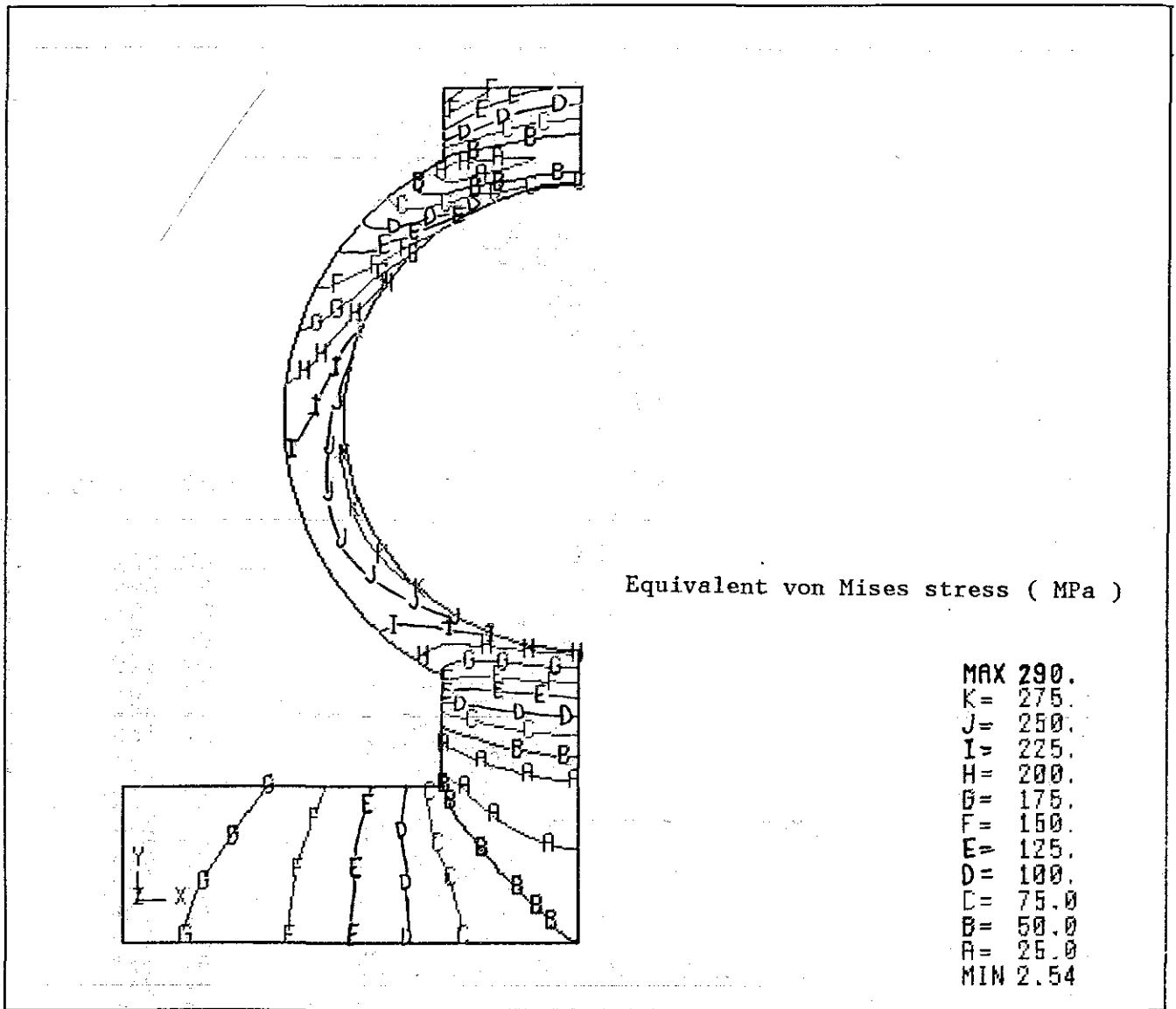


Figure 31. Equivalent von Mises stress contours in steel for the calculation 5.